Published in final edited form as:
J Org Chem. 2013 December 6; 78(23): 11970–11984. doi:10.1021/jo4020112.

Synthesis and Anticancer Activity of all known (−)-Agelastatin Alkaloids

Sunkyu Han[†], **Dustin S. Siegel**[†], **Karen C. Morrison**[‡], **Paul J. Hergenrother**[‡], and **Mohammad Movassaghi**[†]

Mohammad Movassaghi: movassag@mit.edu

[†]Department of Chemistry, Massachusetts Institute of Technology, Cambridge, Massachusetts 02139, USA

[‡]Department of Chemistry, University of Illinois at Urbana-Champaign, Urbana, Illinois 61801, USA

Abstract

The full details for our enantioselective total syntheses of (−)-agelastatins A–F (**1**–**6**), the evolution of a new methodology for synthesis of substituted azaheterocycles, and the first side-by-side evaluation of all known (−)-agelastatin alkaloids against nine human cancer cell lines are described. Our concise synthesis of these alkaloids exploits the intrinsic chemistry of plausible biosynthetic precursors and capitalizes on a late-stage synthesis of the C-ring. The critical copper-mediated cross-coupling reaction was expanded to include guanidine-based systems, offering a versatile preparation of substituted imidazoles. The direct comparison of the anticancer activity of all naturally occurring (−)-agelastatins in addition to eight advanced synthetic intermediates enabled a systematic analysis of the structure activity relationship within the natural series. Significantly, (−)-agelastatin A (**1**) is highly potent against six blood cancer cell lines (20–190 nM) without affecting normal red blood cells (>333 μM). (−)-Agelastatin A (**1**) and (−)-agelastatin D (**4**), the two most potent members of this family, induce dose dependent apoptosis and arrest cells in the G2/M-phase of the cell cycle; however, using confocal microscopy we have determined that neither alkaloid affects tubulin dynamics within cells.

Introduction

The agelastatins are a family of cytotoxic pyrrole-imidazole alkaloids exhibiting a unique tetracyclic framework with four contiguous stereogenic centers on the carbocyclic C-ring (Figure 1). In 1993, Pietra and co-workers first isolated and studied (−)-agelastatins A (**1**) and B (**2**) from the Coral Sea sponge *Agelas dendromorpha*.[1,2] (−)-Agelastatins C (**3**) and D (**4**) were isolated by Molinski and coworkers in 1998 from *Cymbastela* sp. native to the Indian Ocean.[3] In 2010, Al-Mourabit's group isolated (−)-agelastatins E (**5**) and F (**6**) from the New Caledonian sponge *A. dendromorpha*.[4] (−)-Agelastatin A (**1**) was found to exhibit modest anti-neoplastic activity against multiple tumor cell lines.[1,2,5,6] Specifically, (−)-**1** inhibits osteopontin-mediated neoplastic transformation and metastasis. In addition, (1)-**1** causes cells to arrest in the G2/M-phase of the cell cycle; further studies suggested that the

Correspondence to: Mohammad Movassaghi, movassag@mit.edu.

Supporting Information.

General procedures, additional notes concerning our earlier routes to agelastatins A (**1**) and B (**2**) and the rate of C4-deuterium incorporation in (+)-*O*-methyl-pre-agelastatins A (**39**) and D (**53**), tubulin microscopy images of HeLa Cells, crystal structure of desbromomethylester **S20**, and copy of ^{1}H and ^{13}C NMR spectra. This material is available free of charge via the Internet at http://pubs.acs.org.

arrest could be specifically in the G2-phase.[7] Additionally, recent *in vivo* pharmacokinetic studies in mice demonstrated that (−)-agelastatin A (**1**) is able to penetrate into CNS compartments.[6,8] (−)-Agelastatin A (**1**) also exhibits toxicity towards anthropods,[3] and moderately inhibits the glycogen synthase kinase-3β.[5,9]

The agelastatins are the only isolated pyrrole-imidazole alkaloids with C4–C8 and C7–N12 bonds (Figure 1), and are likely derived from linear biogenetic precursors such as clathrodin,[10] hymenidin,[11] or oroidin.[12,13] Kerr and coworkers showed that histidine and ornithine (or proline) are the amino acid precursors for related pyrrole-imidazole alkaloids.[14,15] Prior to our synthetic report of agelastatin alkaloids,[16] there were two hypotheses for the biogenesis of agelastatin A (**1**) from a putative linear precursor.[1a,17]

Its potent biological activities, in conjunction with its intriguing molecular structure, have prompted considerable efforts towards the total synthesis of agelastatin A (**1**).[18] Preceding our report on the enantioselective total synthesis of (−)-agelastatins A–F (**1**–**6**),[16] ten different research groups had reported inventive solutions to the total synthesis of alkaloid **1**.[19] Interestingly, each of these synthetic strategies were contingent on an early introduction of the central C-ring followed by further derivatization to the natural product **1**. Indeed, agelastatin A (**1**) has continued to serve as a source of inspiration for development of new and innovative synthetic solutions as demonstrated by four additional recent syntheses.[20] Distinct from these approaches, our biosynthetically inspired synthetic strategy involved a late stage C-ring formation and enabled the total synthesis of all known (−)-agelastatins (**1**–**6**).[16] Herein, we provide a detailed account of our enantioselective total synthesis of these alkaloids and the development of a key methodology for the synthesis of imidazol-2-one and 2-aminoimidazoles. We also describe the first comparative anticancer activity study of all known (−)-agelastatins (**1**–**6**), with alkaloids (−)-**1** and (−)-**4** being most active, demonstrating *potent and selective activity against human blood cancer cell lines* by inducing apoptotic cell death.

Results and Discussion

Biosynthetic hypothesis of (−)-agelastatin A

Our retrobiosynthetic analysis of (−)-agelastatin A (**1**) is shown in Scheme 1.[16] The key transformation in our planning involved a 5-*exo*-trig cyclization, forming the central carbocyclic C-ring and introducing the desired C4-, C5-, and C8- stereogenic centers in a single step. We anticipated that the key intermediate, pre-agelastatin A (**9**), would be accessed from the tricycle **10** through a late-stage C8-oxidation. Our planning was partly motivated by the structural similarity of tricycle **10** with the natural alkaloid cyclooroidin (**11**), and the potential formation of the imidazolone D-ring of **10** through methylation and hydrolysis of a related aminoimidazole.[21]

Initial synthetic studies toward agelastatin A

Prior to our discovery and the first use of the nucleophilic D-ring imidazolone in synthesis of the C-ring of these alkaloids, we had planned on the use of keto-triazones for the formation of the C4–C8 bond (Scheme 2). We had expected to enable C-ring generation via nucleophilic attack of a C4-enol to a C8 electrophilic derivative of ketone **12** after C8-oxidation. In this early approach, we planned to introduce the AB-bicyclic structure of ketone **12** via an intramolecular conjugate addition of N12[19a] in enone **13** followed by an oxidative aromatization. The potential stereoablative use of L-proline, a known biosynthetic precursor,[14,22] to introduce the C7 stereochemistry of intermediate **12** was of additional interest.

This early synthetic approach to **1** commenced with a Mitsunobu reaction involving L-proline derivative **14** and allylic alcohol **15** followed by Dess–Martin periodinane (DMP) C5-oxidation to give enone **16** in 73% yield over two steps (Scheme 3). Exposure of carbamate **16** to trifluoroacetic acid resulted in the unveiling of the N12 and spontaneous intramolecular conjugate addition to afford pyrrolidine **17** in 85% yield as a 3.3:1 mixture of diastereomers at C7 (major diastereomer shown). This modest level of diastereoselection hinted at possible further refinement of this approach for asymmetric synthesis of lactam **18** based on the C11-stereochemistry of enone **16**. With interest in addressing the key C-ring cyclization, we proceeded with sequential treatment of ketone **17** with DMP to give the corresponding pyrrole derivative (42% yield) possibly through oxidation of the C11-enol tautomer,[23,24] followed by N9-desulfonylation to afford the desired lactam **18** in 84% yield.[25]

While we successfully validated a range of conditions for activation of ketone **18** as a C4-nucleophile,[26] the oxidation of C8 to generate the necessary electrophile **19** (Scheme 3) proved difficult.[27,28] In contrast to significant literature precedent for the oxidation of amines, the oxidation of amides is rare.[29] After examining a wide range of conditions, we found that treatment of lactam **18** with *N*-*t*-butylbenzenesulfinimidoyl chloride[30] in the presence of DBU gave rise to the enamide **20** in 20% yield along with 20% recovery of lactam **18**. Indeed, when ketone **18** was dissolved in methanol-d_4 in the presence of DBU, complete deuterium incorporation at C4 occurred in less than a minute. The more facile oxidation of the lactam **18** at positions other than C8, and a favorable tautomerization of acylimine **19** to the highly stable bicycle **20** (Scheme 3, arrow B) seemed to prevent the desired formation of the C4–C8 bond (Scheme 3, arrow A). Thus, we sought an alternate strategy for the introduction of the C8-hemiaminal functional grouping of lactam **18**.[31]

Our first-generation total synthesis of (±)-agelastatin A

An orthogonal approach to the desired bicyclic hemiaminal ether **21** was the partial reduction of C8-carbonyl of imide **23** (Scheme 4). Moreover, for the formation of the key C4–C8 bond, we planned to use the imidazolone heterocycle as a nucleophile in accord with our retrobiosynthetic analysis (Scheme 1).

Treatment of the known methyl ester **24**[32] with benzylamine and methoxyamine resulted in the formation of imides (±)-**25a** and (±)-**25b** in 86% and 48% yield, respectively (Scheme 5).[32] Each of these imides was obtained as a racemate, reflecting the facile deprotonation of the acidic C7 proton.[33] Imides (±)-**25a** and (±)-**25b** were readily reduced with L-selectride and subsequent treatment with *p*-toluenesulfonic acid yielded hemiaminal ethers (±)-**26a** and (±)-**26b** in 55% and 46% yield (two steps), respectively. The addition of a lithiated[34] triazone intermediate,[26] prepared by treatment of triazone **27** with *s*-butyllithium, to methyl ester (±)-**26a** gave ketone (±)-**28** in 70% yield.[26] Exposure of triazone (±)-**28** to methanolic hydrogen chloride solution led to spontaneous condensative cyclization[35] to form the imidazolone D-ring in 66% yield (Scheme 5).[26]

Imidazolone (±)-**29** was then treated with scandium trifluoromethanesulfonate ($Sc(OTf)_3$) to induce the acyliminium ion formation and subsequent introduction of the C-ring; however, the C8-hydroxy hemiaminal product (±)-**30**, isolated in 36% yield, and pyrrolopyrazinone **31** (<5% yield) were the only observed products (Scheme 6). When hemiaminal (±)-**30** was exposed to dichloromethane and trifluoroacetic acid (TFA) mixture, pyrrolopyrazinone **31** was obtained in quantitative yield. These results suggested that the acyliminium ion intermediate was transiently formed, but was not effectively trapped by the C4 nucleophile. In an attempt to minimize tautomerization of the acyliminium ion under milder, acid-free reaction conditions, we planned to introduce a sulfoxide group at the C8 position. Thus,

imidazolone (±)-**29** was treated with a mixture of ethanethiol, trifluoroacetic acid, and dichloromethane (EtSH:TFA:CH_2Cl_2 = 1:2.5:10) at 23 °C, to give sulfide (±)-**32** (95%), which was oxidized to sulfoxide (±)-**33** in 55% yield upon treatment with sodium periodate (6:4 dr). However, heating a solution of sulfoxide (±)-**33** in acetonitrile resulted in the exclusive formation of pyrrolopyrazinone **31** (Scheme 6).

To minimize any potential adverse steric blocking imparted by the benzyl group in the attempted C4–C8 bond formation (Scheme 6), we turned our attention to keto-triazone (±)-**34**, which was synthesized via the coupling of methyl ester (±)-**26b** and α-lithiated triazone generated from tin-lithium exchange of the organostannane derivative in 74% yield.[26] The keto-triazone (±)-**34** was treated with samarium iodide (73% yield) followed by solvolysis in aqueous hydrochloric acid and methanol mixture to afford imidazolone (±)-**35** (67% yield, Scheme 7). Unfortunately, when imidazolone (±)-**35** was treated with TFA–water mixture in acetonitrile, the elimination of methanol occurred to give pyrrolopyrazinone **36** in 95% yield (Scheme 7).[36]

We were cognizant that the formation of pyrrolopyrazinone **36** was a result of rapid C7-deprotonation of the C8-iminium ion intermediate to generate the conjugated bicycle prior to the trapping of C8-electrophile with C4-nucleophile (Scheme 7). Therefore, we considered substrate modifications that would lower the kinetic acidity of the proton at C7 and provide greater opportunity for the formation of the desired C4–C8 bond. We envisioned that the allylic strain between the C13-bromide and the C6-methylene, present in all agelastatins, might hinder this tautomerization event. Comparison of the calculated minimum energy conformation of the acyliminium ion derived from C8-ionization of **35** and brominated acyliminium ion **8** (Scheme 1) revealed that the H7 of intermediate **8** is ~22° further away from ideal conformation for acidification as compared to that of the nonbrominated acyliminiun ion.[37] Thus the C7-proton of C13-brominated acyliminium ion **8** would be less susceptible to deprotonation as the overlap of C7–H7 σ-orbital with C8–N9 π^*-orbital would be less than that of the nonbrominated acyliminium ion.[38] We envisioned that the lowered kinetic acidity of H7 in the C13-brominated acyliminium ion intermediate **8** would provide greater prospect to trap the C8-electrophilic center with C4-nucleophile before the undesired H7-deprotonation.

This analysis of the possible difference in the preferred H7–C7–C8–H8 dihedral angles of the bromo versus desbromo intermediates prompted us to evaluate the effect of C13-bromide in the key C4–C8 bond forming step. For the introduction of the bromide at C13, keto-triazone **34** was treated with *N*-bromosuccinimide (NBS) to give bromopyrrole **37** in 45% yield (Scheme 8). Samarium iodide–mediated reduction of *N*-methoxylactam **37** (64% yield) followed by treatment with aqueous hydrogen chloride in methanol afforded (±)-*O*-methyl-pre-agelastatin A (**39**) in 65% yield. Gratifyingly, when (±)-*O*-methyl-pre-agelastatin A (**39**) was treated with TFA and water in acetonitrile, (±)-agelastatin A (**1**) and (±)-di-*epi*-agelastatin A (**40**) were obtained as a 2:1 mixture in 47% combined yield.[39] Careful monitoring of this transformation revealed that (±)-4,5-di-*epi*-agelastatin A (**40**) was the kinetic product, which equilibrated to the thermodynamically favored (±)-agelastatin A (**1**). With confirmation of the key step at hand, the synthesis of (±)-*O*-methyl-pre-agelastatin A (**39**) was envisioned to be streamlined via a fragment assembly that would obviate the need for the *N*-methoxy substitution of the B-ring lactam.[37]

Our second-generation total synthesis of (−)-agelastatin A

We rationalized that a facile and reversible enolization at C7 caused the racemization of imide derivatives **25a** and **25b** (Scheme 5). Therefore, similar to our solution for the successful key C4–C8 bond formation (Scheme 8), we envisioned that the bromination at

C13 of these imides would lower the kinetic acidity of their H7 and potentially minimize erosion of their enantiomeric excess.[37] Amide (+)-**41** could be obtained in two steps from a known pyrrole derivative upon bromination and acylation.[16] When amide (+)-**41** was dissolved in methanol-d_4 we observed facile B-ring cyclization.[40] Importantly, it took 1 h for the C7-methine to show 52% deuterium incorporation and an additional 2 hours to show complete deuterium incorporation (Scheme 9), which we reasoned could provide us with a small window of opportunity to intercept the imide carbonyl C8 via a rapid reduction before racemization.

Thus, we exposed methyl ester (+)-**41** to sodium borohydride in methanol at 0 °C (Scheme 10), which led to cyclization and reduction of the resulting imide to afford an α-hydroxyamide intermediate. Subsequent addition of *p*-toluenesulfonic acid monohydrate to the reaction mixture enabled a methanolysis reaction to directly give bicycle (+)-**44** in 90% (>10 g-scale) and 99% ee.

While the C13-bromide served critical roles in both suppressing C7-racemization (Scheme 10) and enabling the key C-ring cyclization (Scheme 8), it was incompatible with the addition of the lithiated triazone to methyl ester (+)-**44** as detailed in Scheme 5. When the same lithiated triazone was exposed to methyl ester (+)-**44**, the reaction was plagued by the undesired reactivity between the C13-bromide and the organolithium species. The corresponding Grignard, organocerium, organocuprate, and organozinc derivatives failed to add to methyl ester (+)-**44**. However, we found that the organocerium triazone derivative added smoothly to an aldehyde variant of ester (+)-**44** for the introduction of the C4–C5 bond (64% yield), enabling our second generation total synthesis of (−)-agelastatins A (**1**) and B (**2**).[37] Following our successful access to enantiomerically enriched alkaloids (−)-**1** and (−)-**2** via strategic introduction of C13-bromide at an early stage of the synthesis, we pursued a more concise strategy for the union of the desired triazone fragment and the readily available bicyclic ester (+)-**44**.

Our third-generation total synthesis of (−)-agelastatins A–F

Inspired by the Liebeskind group's reports on the cross-coupling reaction between thioesters and organostannanes,[41] we set out to develop an efficient metal-mediated cross-coupling reaction between thioester (+)-**45**, derived from methyl ester (+)-**44** in one step,[16] and a stannyl triazone derivative (Table 1).[42] Under the previously reported reaction conditions,[41b] thioester (+)-**45** and triazone **46** in the presence of $Pd_2(dba)_3$, Cu(I) diphenylphosphinate (CuDPP), and triethyl phosphite in THF at 23 °C failed to deliver the desired product (Table 1, entry 1). Substitution of triethyl phosphite with SPhos also showed no improvement (Table 1, entry 2). Interestingly, upon treatment of thioester (+)-**45** and triazone **46** with a catalytic amount of $Pd(PPh_3)_4$ and stoichiometric amount of CuDPP at 50 °C, the desired coupled product (+)-**48** was obtained in 50% yield. Under these conditions, byproduct **49a**, resulting from an undesired transfer of a *n*-butyl group from the stannane **46**, was also formed in 50% yield (Table 1, entry 3). By switching the copper additive to Cu(I)-thiophene-2-carboxylate (CuTC), we could favor the formation of the desired coupled product (+)-**48** (60% yield) over the undesired byproduct **49a** (40% yield, Table 1, entry 4). Notably, this transformation could be carried out with equal efficiency without the palladium catalyst (Table 1, entry 5).[43] The undesired alkyl transfer from stannanes has been reported during transmetallation involving an sp^3-hybridized carbon in the Stille cross-coupling reactions.[44,45] In an attempt to suppress this undesired alkyl transfer, we employed a stannyltriazone substrate **47** containing cyclohexyl groups as auxiliary ligands to the tin.[46] Importantly, when thioester (+)-**45** and triazone **47** were treated with CuTC (1.5 equiv) at 50 °C, the desired ketone (+)-**48** was formed exclusively in 96% yield and 99% ee (>5 g-scale, Table 1, entry 6).

Having established a reliable method to access ketone (+)-**48**, we next focused on the optimization of the final steps leading to (−)-agelastatin A (**1**). We found that keto-triazone (+)-**48** was most efficiently converted to (+)-*O*-methyl-pre-agelastatin A (**39**) upon exposure to methanolic hydrogen chloride at 65 °C (89% yield, 99% ee, Scheme 11). Additionally, treatment of (+)-*O*-methyl-pre-agelastatin A (**39**) with aqueous methanesulfonic acid at 100 °C, followed by introduction of methanol to the resulting mixture of (−)-agelastatin A (**1**) and (−)-di-*epi*-agelastatin A (**40**), afforded (−)-agelastatin A (**1**) in 49% yield (99% ee, >1 g-scale) along with (−)-*O*-methyl-di-*epi*-agelastatin A (**50**, 22% yield, Scheme 11). Not only could diastereomer **50** be readily separated by flash column chromatography, but its resubmission to the above protocol provided another batch of (−)-agelastatin A (**1**) in 66% yield along with recovered (−)-**50** in 30% yield.[47] While treatment of an aqueous tetrahydrofuran solution of (−)-agelastatin A (**1**) with NBS and 2,6-di-*t*-butyl-4-methylpyridine (DTBMP) efficiently afforded (−)-agelastatin B (**2**) in 84% yield, the exposure of a methanolic solution of (−)-**1** to amberlyst 15 resin provided (−)-agelastatin E (**5**) in 96% yield.[1c]

Concerning the synthesis of (−)-agelastatin C (**3**), a wide range of oxidants tested was found to be ineffective for the direct oxidation of the C4-methine of (−)-agelastatin A (**1**). Thus, we devised a strategy based on the oxidation of (−)-dehydroagelastatin A (**51**, Scheme 11). We were pleased to find that (−)-*O*-methyl-di-*epi*-agelastatin A (**50**) could be readily converted to (−)-dehydroagelastatin A (**51**) upon heating in pyridine at 115 °C in 95% yield (Scheme 11). [48] Treatment of (−)-dehydroagelastatin A (**51**) with dimethyldioxirane (DMDO) provided (−)-di-*epi*-agelastatin C (**52**) in 98% yield, via oxidation on the convex face. Notably, heating an aqueous solution of (−)-di-*epi*-agelastatin C (**52**) in the presence of amberlyst 15 resin afforded (−)-agelastatin C (**3**) in 41% yield along with recovered (−)-di-*epi*-agelastatin C (**52**, 42% yield).

Our copper-mediated cross-coupling reaction of thioester and organostannane enabled an efficient synthesis of (+)-*O*-methyl-pre-agelastatin D (**53**, Scheme 12) as described in the following section (Table 2), and consequently the first synthetic sample of (−)-agelastatin D (**4**). While we were pleased to access alkaloid (−)-**4**, this cyclization was plagued by the competing reaction pathways involving the C6–C7 bond cleavage, resulting in byproduct **55** (20% yield) and C4–C13 cyclization, giving byproduct **56** (20% yield).

Interestingly, heating an aqueous acidic solution of 13-desbromoenamide **57** resulted in clean formation of tetracycle **56** (46%).[49] Consistent with this observation, we propose that byproduct **56** is formed via protodebromination at C13, followed by enamide formation, and C4 to C13 cyclization. Since we were unable to confirm the intermediacy of pyrrolopyrazinone **57** in the reaction mixture, we cannot exclude a mechanism involving protodebromination after the C4–C13 cyclization.

The formation of byproducts **55** and **56** are consistent with the lower C4-nucleophilicity of (+)*O*-methyl-pre-agelastatin D (**53**) compared to that of (+)-*O*-methyl-pre-agelastatin A (**39**). Indeed, monitoring of the rates of deuterium incorporation at C4 position of (+)-*O*-methyl-pre-agelastatins A (**39**) and D (**53**), respectively, revealed that deuterium incorporation at C4 occurred ten times faster in (+)-**39** as compared to (+)-**53** (k_1=3.094 × 10^{-5}/sec, k_2=3.028 × 10^{-6}/sec),[37] consistent with its more efficient C4–C8 bond formation (Scheme 14). It is interesting to note that the scarcity of natural (−)-agelastatin D (**4**) compared to other N1-methyl agelastatin alkaloids is consistent with this observation on the lower efficiency of the desired cyclization with **53** as compared to **39**.[50]

Copper-mediated cross-coupling reaction of thioesters and organostannanes: Expanded scope and application

The successful copper-mediated cross-coupling reactions between thioester **45** and organostannanes **46** and **47** (Table 1) prompted our examination of its scope and potential broader application (Scheme 15). Of particular interest was the possible general use of this methodology to allow synthesis of versatile ketone **62** by formation of the C1–C2 bond from thioester **60** and organostannane **61** (X=O or NR). We envisioned that condensative cyclization of the urea or guanidine function of intermediate **62** on to the C1-carbonyl would provide an expeditious route to the corresponding imidazol-2-one (X=O) or related azaheterocycle **63**, common substructures in various natural products.[17]

Our cross-coupling reaction was effective for both alkyl and aryl thioester coupling partners. Both cyclohexanecarbonyl thioester **64** and benzoyl thioester **65** underwent efficient cross-coupling with stannyl triazone **47** to give the corresponding ketones **71** and **72** in 95% and 99% yield, respectively (Table 2, entries 1 and 2). Consistent with our prior observation (Table 1), the use of organostannane **46**, containing *n*-butyl auxiliary ligands, as a coupling partner resulted in lower yield (Table 2, entry 3) due to competitive formation of the undesired *n*-butyl ketone byproduct. Stannyl guanidine **67**[37] proved to be highly effective for the introduction of the guanidine functionality as illustrated through its cross-coupling with thioesters **65** and **66**, affording the corresponding ketones **73** and **75**, respectively (Table 2, entries 4 and 6). Importantly, ketones **73** and **75** could be readily converted to the corresponding 2-aminoimidazoles in quantitative yield upon treatment with TFA and warming, highlighting the synthetic utility of our method as a means to generate 2-aminoimidazoles (Table 2, entries 5 and 7). Stannyl triazone **68** was found to undergo smooth coupling with adipic thioester **66** to provide diketone **77** in 82% yield (Table 2, entry 8). Gratifyingly, under our standard reaction condition, the stannyl urea **69** was found to afford the desired cross-coupling with the complex thioester (+)-**45** to give the corresponding ketone, which after treatment with methanolic hydrogen chloride at 65 °C provided (+)-*O*-methyl-pre-agelastatin A (**39**, 58% yield and 99% ee, Table 2, entry 9).[16] This direct coupling between thioester (+)-**45** and stannyl urea **69** enabled us to further streamline our synthesis of (−)-agelastatin A (**1**) to seven steps from commercially available material.[16] Similarly, (+)-*O*-methyl-pre-agelastatin D (**53** Table 2, entry 10)[16] could be prepared from thioester (+)-**45** and urea **70** in 62% yield (2 steps), which enabled the first synthetic access to (−)-agelastatin D (**4**, *vide supra*). The efficient union of a variety of aminostannanes and thioester fragments and subsequent direct conversion of the keto-triazone and keto-guanidine intermediates to the corresponding imidazolones and aminoimidazoles is promising for future application of this chemistry to the synthesis of other oroidin based natural products such as cyclooroidin (**11**), nagelamides, sceptrins, and many other derivatives.[51]

Anticancer activity and structure–activity relationship studies

The enantioselective total synthesis of all six (−)-agelastatin alkaloids (**1**–**6**), as well as eight structurally-related alkaloids and advanced intermediates, provided an opportunity to further probe the structure–activity relationship for this class of natural products. Significantly, we set out to provide the first comparative anticancer activity study involving all natural members of this family of alkaloids in five human cell lines. Previous reports have tested the activity of (−)-agelastatin A (**1**) relative to other available derivatives in a single cell line, showing that structural changes do affect the activity;[1a,1c,3,4] however, no comprehensive comparison of the entire class of agelastatins against multiple cell lines has been performed. Furthermore, although (−)-agelastatin A (**1**) has been characterized for its anti-neoplastic activity in a range of cancer types, including leukemia, prostate, breast, colon, uterine, pancreatic, lung, and others,[1a,1c,2–7] the heterogeneity across these studies makes it

impossible to make a true assessment of selectivity for any one type of cancer. We sought to refine the structure-activity relationship of this class with our complete panel of (−)-agelastatins A–F (**1**–**6**, respectively) and test it more broadly against a range of cancer cell lines.

While this total synthesis program generated more than four dozen compounds for testing, after a preliminary examination in HeLa and U-937 cells indicated many were completely inactive, we decided to focus extensively on the six natural (−)-agelastatins along with eight closely related derivatives that either bear the tetracyclic framework or are immediate precursors to the complex alkaloids (Table 3). The six (−)-agelastatin alkaloids (**1**–**6**, respectively), (−)-*O*-methyl-di-*epi*-agelastatin A (**50**), (−)-dehydroagelastatin A (**51**), (−)-di-*epi*-agelastatin C (**52**), (+)-*O*-methyl-pre-agelastatin A and D (**39** and **53**, respectively), along with bicyclic pyrroles (+)-**44**, (+)-**45**, and triazone (+)-**48** were tested for their ability to induce cell death in four human cancer cell lines (U-937, lymphoma; HeLa, cervical carcinoma; A549, non-small cell lung carcinoma; and BT549, breast carcinoma) and one immortalized normal human cell line (IMR90, lung fibroblasts) after a 48-hour exposure.[37] As shown in Table 3, (−)-agelastatin A (**1**) exhibited the highest potency in all cell lines tested, whereas (−)-agelastatins C (**3**) and F (**6**) showed no activity at the concentrations examined. Furthermore, we observed an enhanced activity of (−)-agelastatin A (**1**) in U-937 (20×) and BT549 (4×) cells relative to the other cell lines (Table 3). (−)-Agelastatin D (**4**), which lacks a methyl group on the D-ring, also showed reasonable activity against U-937 cells and modest activity against BT549 cells. This activity was selective relative to the other cell lines, and follows a similar trend in activity to that of (−)-agelastatin A (**1**). (−)-Agelastatin B (**2**) and (−)-agelastatin E (**5**) showed weak activity, albeit with the same overall pattern as alkaloids (−)-**1** and (−)-**4**. Furthermore, none of the *epi*-agelastatin derivatives [(−)-**50** or (−)-**52**], *O*-methyl-pre-agelastatins [(+)-**39** or (+)-**53**], dehydroagelastatin (−)-**51** or any of structurally simpler derivatives [(+)-**44**, (+)-**45**, or (+)-**48**] showed any activity at the concentrations tested against these cell lines (Table 3).

Together, this set of data allows the first direct comparison of all naturally occurring agelastatin alkaloids and suggest that the stereochemistry for the imidazolidinone ring is crucial [compare (−)-**5** vs. (−)-**50**] while addition of the C14-bromide substituent to the pyrrole is detrimental to activity (5–20 fold reduction) of the agelastatins [compare (−)-**1** vs. (−)-**2**, and (−)-**4** vs. (−)-**6**]. Demethylation of the imidazolidinone ring gives more modest reductions (1–5 fold reductions) in anticancer potency as seen by comparing (−)-agelastatin A (**1**) and (−)-agelastatin D (**4**). Methylation of the C5-hydroxyl reduces the activity by >10 fold as evident by comparing (−)-agelastatin A (**1**) and (−)-agelastatin E (**5**). Finally, C4-hydroxylation completely abolishes activity as demonstrated by comparing (−)-agelastatin A (**1**) and (−)-agelastatin C (**3**). The observed necessity of alkylation of the imidazolidinone ring is consistent with previous report,[7] which have also indicated that chlorination rather than bromination does not affect activity.

Anticancer activity of (−)-agelastatins A–F in blood cancer cell lines

Based on the exceptional potency of (−)-agelastatins A (**1**) and D (**4**) against U-937 cells relative to the other cell lines tested, five additional blood cancer cell lines were tested for their sensitivity to the agelastatin alkaloids. These cell lines spanned a variety of cancer types (CEM, acute lymphoblastic leukemia; Jurkat, acute T-cell leukemia; Daudi, Burkitt's lymphoma; HL-60, acute promyelocytic leukemia; CA46, Burkitt's lymphoma). After a 48-hour incubation, the ability of (−)-agelastatins A–F (**1**–**6**) to induce cell death was evaluated. As shown in Table 4, all five cell lines showed remarkable sensitivity to (−)-agelastatin A (**1**). The same trends in potency observed for the various agelastatins with the general cell panel (Table 3) were also observed. These results, *the first indication of heightened potency*

*of **1** versus a panel of white blood cell cancer cell lines*, highlight the outstanding potential for the use of agelastatin A (**1**) against blood cancers.[52] This is especially encouraging, given the difficulty of treating blood cancers clinically.[53]

Hemolytic activity of (−)-agelastatins A–F and advanced intermediates

To further explore the translational potential of the agelastatin alkaloids, all fourteen compounds in Table 3 were evaluated for their hemolytic activity (Figure 2). Notably, none of the active agelastatin alkaloids [(−)-**1**, (−)-**2**, (−)-**4**, or (−)-**5**] show any nonspecific hemolysis of red blood cells. The triazone derivative (+)-**48** showed some hemolytic activity; however, this compound was completely inactive in all cell lines tested (Table 3). In light of the exceptional potency of (−)-agelastatin A (**1**) against a range of blood cancer cell lines, this high degree of selectivity strongly suggests further translational studies are warranted.

Apoptotic activity of (−)-agelastatins A and D

We next sought to determine whether the most active (−)-agelastatins A (**1**) and D (**4**) induce apoptotic cell death. In apoptosis a cascade of events results in the activation of procaspase-3, a low activity zymogen, to caspase-3, a cysteine protease that cleaves scores of cellular substrates resulting in cell death.[54] A hallmark of cancer is a resistance to apoptosis,[55] thus, compounds that are able to induce apoptotic death in cancer cells are interesting mechanistically and have potential as chemotherapeutics. Experimentally, apoptosis is most readily detected through a) the observation of procaspase-3 (PC3) maturation to caspase-3 (C3), b) the cleavage of caspase-3 substrates, most notably the enzyme PARP-1, and c) the exposure of phosphatidyl serine of the exterior cell membrane before loss of membrane integrity.[56] Procaspase-3 maturation and PARP-1 cleavage can readily be detected via Western blotting, and phosphatidyl serine exposure is detected by antibody staining and flow cytometry. Concentrations of agelastatins A (**1**) and D (**4**) in these experiments were chosen to provide a robust response after 24 hr. Therefore, the compounds were tested at 2×, 4×, and 6× concentration relative to their IC_{50} determination experiment, which were performed after 48 h.[57] As shown in Figure 3, (−)-agelastatins A (**1**) and D (**4**) induced dose-dependent activation of procaspase-3 to active caspase-3, and cleavage of PARP-1, consistent with apoptosis.

We next examined whether (−)-agelastatins A (**1**) and D (**4**) induced phosphatidylserine exposure prior to membrane permeabilization. This was determined by evaluating the timing of FITC-labeled annexin-V to the phosphatidylserines relative to the incorporation of propidium iodide, a DNA stain that can only enter dead cells. Concentrations of agelastatins A (**1**) and D (**4**) were chosen to provide a robust response after 21 hr. Therefore, the compounds were tested at 4× and 6× concentration relative to their IC_{50} determination experiment, which were performed after 48 h.[57] As shown by the scatterplots in Figure 4, the number of apoptotic cells (lower right quadrant in Figure 4) increases with dose of compound. These results show, for the first time, that these compounds induce apoptotic death of cancer cells.

Cell cycle arrest with (−)-agelastatins A and D

After establishing apoptotic induction by (−)-agelastatins A (**1**) and D (**4**), experiments were conducted to probe the ability of these compounds to induce cell cycle arrest in U-937 cells. As shown in Figure 5, both compounds induced arrest in the G2/M phase mirroring prior findings[7] related to (−)-**1** and now demonstrating a direct relevance to the activity of (−)-agelastatin D (**4**). Significantly, while arrest in the G2/M phase is commonly associated with disruption of microtubules within the cell,[58] using confocal microscopy, we have

determined that neither (−)-agelastatin A (**1**) nor (−)-agelastatin D (**4**) affects tubulin dynamics within cells (Figure S4).[59] Microtubule stabilization or destabilization results in heightened or reduced levels of tubulin fluorescence, respectively, as shown with the known tubulin binders Taxol and colchicine. Treatment with (−)-agelastatins A (**1**) and D (**4**) results in no change in tubulin fluorescence, an experimental observation consistent with a prior hypothesis regarding their mode of action.[7]

Conclusions

We describe the development of a concise, stereocontrolled, and biosynthetically inspired synthetic strategy toward the agelastatin alkaloids, the development a versatile new synthetic methodology for azaheterocycle synthesis, and its successful implementation to the synthesis of all known (−)-agelastatins (**1**–**6**) and many derivatives. In addition we describe the first comparative study of the anticancer activity of all known agelastatin alkaloids. Key features of our syntheses include: 1) the early introduction of C13-bromide to suppress C7-enolization, 2) the development of a CuTC-mediated cross-coupling reaction between thioester and organostannane, 3) a new [4+1] annulation approach for the synthesis of imidazolones and related azaheterocycles, and 4) the validation of our bioinspired use of the imidazolone for an advanced stage C-ring formation, C4–C8 bond formation and introduction of three stereogenic centers. The efficiency of our synthetic sequence was highlighted by >1 gram batch preparation of (−)-agelastatin A (**1**). The generality of our synthesis allowed for the first side-by-side testing of all known agelastatin alkaloids for their ability to induce cell death in U-937 (lymphoma), HeLa, (cervical carcinoma), A549 (non-small cell lung carcinoma), BT549 (breast carcinoma), and IMR90 (immortalized lung fibroblasts) human cell lines. (−)-Agelastatin A (**1**) exhibited the highest potency in all cell lines tested while (−)-agelastatin D (**4**) retained antineoplastic activity, albeit at a 4-fold lower potency than that of (−)-(**1**). Our results show, for the first time, that both (−)-agelastatins A and D induce apoptotic death of cancer cells and that neither affects tubulin dynamics within cells. We also show that both of these molecules arrested cell growth in the G2/M phase. The exceptional potency of (−)-agelastatins A (**1**) and D (**4**) against U-937 cells led us to investigate all agelastatins (**1**–**6**) in five additional human blood cancer cell lines (Table 4). From these studies, we found that (−)-agelastatins A (**1**) is highly potent against these blood cancer cell lines (20–190 nM) without affecting normal red blood cells (>333 μM). These compounds are particularly active against white blood cancer cell lines, and the selectivity for these cells over normal cells suggests considerable potential as anticancer agents.

Experimental Section

Information for Key Compounds

For complete experimental procedures and full characterization data for all (−)-agelastatin alkaloids A–F (**1**–**6**, respectively) in addition to the eight advanced derivatives (+)-**39**, (+)-**44**, (+)-**45**, (+)-**48**, (−)-**50**, (−)-**51**, (−)-**52**, and (+)-**53** examined in our anticancer activity assays, please see the supporting information of our previous report of the total synthesis of all (−)-agelastatins.[16] For complete experimental procedures and full characterization data for the key compounds (+)-**41**, **47**, (−)-**54**, **55**, and (±)-**56** discussed in our fully optimized route, please see the supporting information of our previous report of the total synthesis of all (−)-agelastatins.[16] For complete experimental procedures and full characterization data for all new substrates and products reported in Table 3, please see below.

***S*,*S*-Di-*p*-tolyl hexanebis(thioate) 66—**To a flask charged with adipic acid (4.0 g, 27 mmol, 1 equiv) was added thionyl chloride (5.0 mL, 68 mmol, 2.5 equiv) and the reaction

flask was equipped with a reflux condensor and heated to 85 °C (The exhaust gases were passed through a 5 N aqueous potassium hydroxide solution). After 1.5 h, the reaction mixture was allowed to cool to 23 °C and concentrated under reduced pressure to afford acyl chloride derivative as a viscous oil.[60] The resulting crude material was dissolved in dichloromethane (10 mL) and the resulting mixture was transferred to a solution of 4-methyl-benzenethiol (7.3 g, 57 mmol, 2.1 equiv) in dichloromethane (30 mL) via cannula at 0 °C. The reaction mixture was allowed to gently warm to 23 °C. After 2 h, triethylamine (2.0 mL, 14 mmol, 0.52 equiv) was added to the reaction mixture. After 25 min, more triethylamine (3.0 mL, 22 mmol, 0.79 equiv) was added to the reaction mixture. After 16.5 h, the reaction mixture was diluted with dichloromethane (210 mL) and saturated aqueous sodium bicarbonate solution (250 mL) and the layers were separated. The aqueous layer was extracted with dichloromethane (250 mL), and the combined organic layers were dried over anhydrous sodium sulfate, were filtered, and were concentrated under reduced pressure. The residue was purified by flash column chromatography (silica gel: diam. 9.0 cm, ht. 12 cm; eluent: 11% ethyl acetate in hexanes) to afford thioester **66** (4.6 g, 47%) as a white solid; mp 105–107°C. ^{1}H NMR (500 MHz, $CDCl_3$, 21 °C): δ 7.27 (app-d, *J* = 8.1 Hz, 4H), 7.20 (app-d, *J* = 7.9 Hz, 4H), 2.67–2.64 (m, 4H), 2.36 (s, 6H), 1.78–1.75 (m, 4H). ^{13}C NMR (125.8 MHz, $CDCl_3$, 21 °C): δ 197.7, 139.9, 134.6, 130.2, 124.3, 43.2, 25.0, 21.5. FTIR (neat) cm^{-1}: 2929 (m), 1687 (s), 1493 (m), 1034 (m), 813 (s). HRMS (ESI, TOF) (*m*/*z*): calc'd for $C_{20}H_{22}NaO_2S2$, $[M+Na]^+$: 381.0959, found: 381.0965. TLC (17% ethyl acetate in hexanes), R*f*: 0.53 (CAM, UV).

1-((Tricyclohexylstannyl)methyl)-*N*,*N*′-di-*tert*-butylcarbamoylguanidine (67)— (tricyclohexylstannyl)methanamine (910 mg, 2.28 mmol, 1 equiv) was dissolved in acetonitrile (60 mL), and (*E*)-*tert*-butyl(((*tert*-butoxycarbonyl)imino)(1*H*-pyrazol-1-yl)methyl)carbamate (1.09 g, 3.43 mmol, 1.50 equiv) was added sequentially at 23 °C. After 11 h, the resulting mixture was concentrated under reduced pressure, and the crude residue, adsorbed onto silica gel, was purified by flash column chromatography (silica gel: diam. 4.0 cm, ht. 12 cm; eluent: 3.3% ethyl acetate in hexanes) to afford tricyclohexyltin reagent **67** (1.3 g, 91%) as a white amorphous residue. ^{1}H NMR (500 MHz, $CDCl_3$, 21 °C): δ 11.39 (s, 1H), 8.44 (t, *J* = 5.1 Hz, 1H), 3.08 (d, *J* = 5.6 Hz, 2H), 1.84 (t, *J* = 4.4 Hz, 6H), 1.62 (d, *J* = 9.6 Hz, 9H), 1.53 (t, *J* = 7.1 Hz, 9H), 1.48 (s, 9H), 1.45 (s, 9H), 1.28–1.21 (m, 9H). ^{13}C NMR (125.8 MHz, $CDCl_3$, 21 °C): δ 163.9, 155.8, 153.6, 82.9, 78.9, 32.4, 29.5, 28.6, 28.2, 27.5, 27.4, 24.1. FTIR (neat) cm^{-1}: 3327 (s), 2917 (s), 2846 (s), 1717 (s), 1642 (s), 1575 (s), 1409 (s), 1337 (s), 1157 (s), 1052 (s), 909 (m), 735 (m). HRMS (ESI, TOF) (*m*/*z*): calc'd for $C_{30}H_{56}N_3O_4Sn$, $[M+H]^+$: 642.3293, found: 642.3290. TLC (10% ethyl acetate in hexanes), R*f*: 0.56 (CAM).

5-Benzyl-1-methyl-3-((tricyclohexylstannyl)methyl)-1,3,5-triazinan-2-one (68)— To a solution of triazone 5-benzyl-1,3-dimethyl-1,3,5-triazinan-2-one (1.5 g, 6.8 mmol, 2.0 equiv) in tetrahydrofuran (40 mL) at −78 °C was added *sec*-butyllithium (1.4 M in cyclohexane, 4.9 mL, 6.8 mmol, 2.0 equiv) via syringe to result in an orange homogeneous solution. After 5 min, a solution of tricyclohexyltin chloride (1.42 g, 3.42 mmol, 1 equiv) in tetrahydrofuran (10 mL) at −78 °C was transferred to the resulting bright orange mixture via cannula over a 3 min period. After 8 min, saturated aqueous ammonium chloride solution (5 mL) was added via syringe. The resulting mixture was partitioned between dichloromethane (250 mL) and water (200 mL). The layers were separated, the aqueous layer was extracted with dichloromethane (250 mL), and the combined organic layers were dried over anhydrous sodium sulfate, were filtered, and were concentrated under reduced pressure. The crude residue was purified by flash column chromatography (silica gel: diam. 5 cm, ht. 10 cm; eluent: hexanes then 17% ethyl acetate in hexanes) to afford stannyltriazone **68** (1.8 g, 90%) as a white amorphous residue. ^{1}H NMR (500 MHz, $CDCl_3$, 21 °C): δ 7.34–7.24 (m,

5H), 4.10 (s, 2H), 4.03 (s, 2H), 3.90 (s, 2H), 2.81 (s, 3H), 2.75 (s, 2H), 1.84 (dd, *J* = 12.5, 2.0 Hz, 3H), 1.63 (d, *J* = 8.9 Hz, 12H), 1.55–1.39 (m, 6H), 1.31–1.17 (m, 12H). ^{13}C NMR (125.8 MHz, $CDCl_3$, 21 °C): δ 156.1, 137.9, 129.1, 128.7, 127.7, 69.7, 67.6, 55.8, 32.9, 32.4, 29.5, 29.0, 27.9, 27.4. FTIR (neat) cm^{-1}: 2917 (s), 2229 (m), 1634 (s), 1519 (s), 1445 (s), 1408 (m), 1297 (s), 1144 (m), 908 (s), 735 (s). HRMS (ESI, TOF) (*m*/*z*): calc'd for $C_{30}H_{50}N_3OSn$, $[M+H]^+$: 588.2987, found: 588.2976. TLC (17% ethyl acetate in hexanes), R*f*: 0.32 (CAM, UV).

1-(2-Cyclohexyl-2-oxoethyl)-3-methyl-5-(*p*-tolyl)-1,3,5-triazinan-2-one (71)— Anhydrous tetrahydrofuran (1.0 mL, degassed thoroughly by passage of a stream of argon) was added via syringe to a flask charged with thioester **64** (12.0 mg, 51.2 μmol, 1 equiv), triazone **47**[16] (36.0 mg, 61.4 μmol, 1.20 equiv), and copper(I)-thiophene-2-carboxylate (CuTC, 15.3 mg, 76.8 μmol, 1.50 equiv) at 23 °C under an argon atmosphere, and the reaction mixture was heated to 50 °C. After 1 h, the reaction mixture was allowed to cool to 23 °C and was filtered through a plug of celite with ethyl acetate washings (3 × 1 mL). The resulting mixture was partitioned between ethyl acetate (20 mL) and saturated ammonium chloride aqueous solution (20 mL). The aqueous layer was extracted with ethyl acetate (2 × 20 mL), and the combined organic layers were dried over anhydrous sodium sulfate, and were concentrated under reduced pressure. The crude residue was purified by flash column chromatography (silica gel: diam. 2 cm, ht. 10 cm; eluent: 25% ethyl acetate in hexanes) to afford ketotriazone **71** (16 mg, 95%) as a colorless oil. ^{1}H NMR (500 MHz, $CDCl_3$, 21 °C): δ 7.08 (d, *J* =8.0 Hz, 2H), 6.94 (d, *J* =8.6 Hz, 2H), 4.69 (s, 2H), 4.66 (s, 2H), 4.09 (s, 2H), 2.88 (s, 3H), 2.32 (tt, *J* =11.4, 3.4 Hz, 1H), 2.27 (s, 3H), 1.80 (dd, *J* = 13.3, 2.2 Hz, 2H), 1.76–1.72 (m, 2H), 1.66–1.60 (m, 2H), 1.32 (ddd, *J* = 15.2, 12.4, 3.1 Hz, 2H), 1.25–1.15 (m, 2H). ^{13}C NMR (125.8 MHz, $CDCl_3$, 21 °C): δ 210.4, 156.1, 146.0, 132.6, 130.1, 119.8, 67.4, 67.4, 53.5, 48.2, 32.4, 28.4, 25.9, 25.7, 20.8. FTIR (neat) cm^{-1}: 2929 (s), 2855 (m), 1720 (m), 1647 (s), 1514 (s), 1300 (m), 1198 (m), 829 (m). HRMS (ESI, TOF) (*m*/*z*): calc'd for $C_{19}H_{26}N_3O_2$, $[M-H]^-$: 328.2025, found: 328.2030. TLC (ethyl acetate), R*f*: 0.40 (CAM).

1-Methyl-3-(2-oxo-2-phenylethyl)-5-(*p*-tolyl)-1,3,5-triazinan-2-one (72)— Anhydrous tetrahydrofuran (1.1 mL, degassed thoroughly by passage of a stream of argon) was added via syringe to a flask charged with thioester **65** (12.0 mg, 52.6 μmol, 1 equiv), triazone **47**[61] (37.0 mg, 63.1 μmol, 1.20 equiv), and copper(I)-thiophene-2-carboxylate (CuTC, 15.7 mg, 78.8 μmol, 1.50 equiv) at 23 °C under an argon atmosphere, and the reaction mixture was heated to 50 °C. After 1 h, the reaction mixture was allowed to cool to 23 °C and was filtered through a plug of celite with ethyl acetate washings (3 × 1 mL). The resulting mixture was partitioned between ethyl acetate (20 mL) and saturated ammonium chloride aqueous solution (20 mL). The aqueous layer was extracted with ethyl acetate (2 × 20 mL), and the combined organic layers were dried over anhydrous sodium sulfate, were filtered, and were concentrated under reduced pressure. The crude residue was purified by flash column chromatography (silica gel: diam. 2 cm, ht. 10 cm; eluent: 25% ethyl acetate in hexanes) to afford ketotriazone **72** (17 mg, 99%) as a colorless oil. ^{1}H NMR (500 MHz, $CDCl_3$, 21 °C): δ 7.92 (dd, *J* = 8.4, 1.2 Hz, 2H), 7.55 (tt, *J* = 7.4, 1.2 Hz, 1H), 7.42 (app-t, *J* = 7.8 Hz, 2H), 7.07 (d, *J* = 8.0 Hz, 2H), 6.95 (app-d, *J* = 8.5 Hz, 2H), 4.80 (s, 2H), 4.73 (s, 2H), 4.72 (s, 2H), 2.92 (s, 3H), 2.28 (s, 3H). ^{13}C NMR (125.8 MHz, $CDCl_3$, 21 °C): δ 196.1, 156.1, 145.9, 135.2, 133.8, 132.6, 130.1, 128.9, 128.3, 119.8, 67.4, 67.3, 52.5, 32.5, 20.3. FTIR (neat) cm^{-1}: 2888 (m), 1694 (m), 1638 (s), 1513 (s), 1288 (m), 1219 (m), 750 (m). HRMS (ESI, TOF) (*m*/*z*): calc'd for $C_{19}H_{20}N_3O_2$, $[M-H]^-$: 322.1556, found: 322.1562. TLC (ethyl acetate), R*f*: 0.46 (CAM, UV).

(*E*)-1,2-Diboc-3-(2-oxo-2-phenylethyl)guanidine (73)—Anhydrous tetrahydrofuran (6.0 mL, degassed thoroughly by passage of a stream of argon) was added via syringe to a flask charged with thioester **65** (36.6 mg, 0.160 mmol, 1 equiv), stannylguanidine **67** (113 mg, 0.176 mmol, 1.10 equiv), and copper(I)-thiophene-2-carboxylate (CuTC, 32.8 mg, 0.165 mmol, 1.03 equiv) at 23 °C under an argon atmosphere, and the reaction mixture was heated to 50 °C. After 1 h, the reaction mixture was allowed to cool to 23 °C, and 5% ammonium hydroxide aqueous solution (15 mL) was added to the reaction mixture. The resulting mixture was extracted with dichloromethane (2 × 15 mL), and the combined organic layers were dried over anhydrous sodium sulfate, were filtered, and were concentrated under reduced pressure. The crude residue was purified by flash column chromatography (silica gel: diam. 2.5 cm, ht. 15 cm; eluent: 11% ethyl acetate in hexanes) to afford ketoguanidine **73** (58 mg, 96%) as a white foam; mp 75–78 °C. ^{1}H NMR (500 MHz, $CDCl_3$, 21 °C): δ 11.5 (s, 1H, NH), 9.41 (s, 1H, NH), 7.98 (dd, *J* = 8.5, 1.2 Hz, 2H), 7.59 (tt, *J* = 7.4, 1.3 Hz, 1H), 7.46 (app-t, *J* = 7.7 Hz, 1H), 4.92 (d, *J* = 4.1 Hz, 2H), 1.51 (s, 9H), 1.50 (s, 9H). ^{13}C NMR (125.8 MHz, $CDCl_3$, 21 °C): δ 193.4, 163.5, 156.1, 153.1, 134.4, 134.3, 129.1, 128.3, 83.5, 79.8, 48.4, 28.4, 28.3. FTIR (neat) cm^{-1}: 3319 (m), 2980 (m), 1727 (s), 1697 (m), 1642 (s), 1618 (s), 1409 (m), 1308 (s), 1148 (s), 734 (m). HRMS (ESI, TOF) (*m*/*z*): calc'd for $C_{19}H_{28}N_3O_5$, $[M+H]^+$: 378.2029, found: 378.2035. TLC (20% ethyl acetate in hexanes), R*f*: 0.44 (CAM, UV).

2-Amino-5-phenyl-1*H*-imidazol-3-ium 2,2,2-trifluoroacetate (74)—To a flask charged with ketoguanidine **73** (57.9 mg, 0.153 mmol, 1 equiv) was added toluene (4 mL) and trifluoroacetic acid (120 μL, 1.53 mmol, 10.0 equiv) via syringe and the reaction mixture was heated to 85 °C. After 13.5 h, the reaction mixture was allowed to cool to 23 °C and was concentrated under reduced pressure. Water (2 mL) and trifluoroacetic acid (120 μL, 1.53 mmol, 10.0 equiv) were added via syringe to the residue and the resulting mixture was heated to 85 °C. After 1.5 h, the reaction mixture was allowed to cool to 23 °C and was concentrated under reduced pressure to give 2-aminoimidazole **74** (34 mg, 82%) as a pale yellow solid; mp 154–156 °C. ^{1}H NMR (500 MHz, CD_3OD, 21 °C): δ 7.56 (app-d, *J* = 7.2 Hz, 2H), 7.43 (app-t, *J* = 7.7 Hz, 2H), 7.34 (app-tt, *J* = 7.4, 1.2 Hz, 1H), 7.13 (s, 1H). ^{13}C NMR (125.8 MHz, CD_3OD, 21 °C): δ 163.1, 149.7, 130.3, 129.7, 129.2, 129.1, 125.6, 109.9, 101.4. FTIR (neat) cm^{-1}: 3182 (br-s), 1682 (br-s), 1204 (s), 1139 (s), 842 (m). HRMS (ESI, TOF) (*m*/*z*): calc'd for $C_9H_{10}N_3$, $[M+H]^+$: 160.0869, found: 160.0867.

(*E*,*E*)-1,1′-(2,7-Dioxooctane-1,8-diyl)bis(2′,3-dibocguanidine) (75)—Anhydrous tetrahydrofuran (34 mL, degassed thoroughly by passage of a stream of argon) was added via syringe to a flask charged with thioester **66** (300 mg, 0.836 mmol, 1 equiv), stannylguanidine **67** (1.34 g, 2.09 mmol, 2.50 equiv), and copper(I)-thiophene-2-carboxylate (CuTC, 374 mg, 1.88 mmol, 2.25 equiv) at 23 °C under an argon atmosphere, and the reaction mixture was heated to 50 °C. After 1 h, the reaction mixture was allowed to cool to 23 °C. The resulting mixture was partitioned between dichloromethane (145 mL) and 5% ammonium hydroxide aqueous solution (145 mL). The aqueous layer was extracted with dichloromethane (3 × 145 mL), and the combined organic layers were dried over anhydrous sodium sulfate, were filtered, and were concentrated under reduced pressure. The crude residue was purified by flash column chromatography (silica gel: diam. 4 cm, ht. 10 cm; eluent: 11% ethyl acetate in hexanes) to afford ketoguanidine **75** (549 mg, 100%) as a white foam; mp 133–136 °C. ^{1}H NMR (500 MHz, $CDCl_3$, 21 °C): δ 11.37 (s, 2H), 9.02 (s, 2H), 4.28 (d, *J* = 4.3 Hz, 4H), 2.42 (app-s, 4H), 1.60 (t, *J* = 3.1 Hz, 4H), 1.47 (s, 9H), 1.46 (s, 9H). ^{13}C NMR (125.8 MHz, $CDCl_3$, 21 °C): δ 203.9, 163.4, 155.9, 153.0, 83.5, 79.7, 51.0, 39.9, 28.4, 28.2, 23.1. FTIR (neat) cm^{-1}: 3319 (br-m), 2980 (m), 2253 (w), 1726 (s), 1643 (s), 1618 (s), 1408 (m), 1309 (s), 1151 (s), 1058 (m), 734 (m). HRMS (ESI, TOF) (*m*/*z*):

calc'd for $C_{30}H_{53}N_6O_{10}$, $[M+H]^+$: 657.3823, found: 657.3801. TLC (50% ethyl acetate in hexanes), R*f*: 0.44 (CAM).

4,4′-(Butane-1,4-diyl)bis(2-amino-1*H*-imidazol-3-ium) 2,2,2-trifluoroacetate (76)—Toluene (40 mL) and trifluoroacetic acid (650 μL, 8.36 mmol, 10.0 equiv) were added via syringe to a flask charged with ketoguanidine **75** (549 mg, 0.836 mmol, 1 equiv) and the resulting mixture was heated to 75 °C. After 16 h, the reaction mixture was allowed to cool to 23 °C and was concentrated under reduced pressure. Water (20 mL) and trifluoroacetic acid (650 μL, 8.36 mmol, 10.0 equiv) were added via syringe to the residue and the resulting mixture was heated to 100 °C. After 45 h, the reaction mixture was allowed to cool to 23 °C and was concentrated under reduced pressure to give 2-aminoimidazole **76** (375 mg, 100%) as a brown solid; mp 200–203 °C. ^{1}H NMR (500 MHz, CD_3OD, 21 °C): δ 6.49 (s, 2H), 2.53 (app-t, *J* = 6.5 Hz, 4H), 1.65 (app-t, *J* = 7.1 Hz, 4H). ^{13}C NMR (125.8 MHz, CD_3OD, 21 °C): δ 162.6, 148.8, 128.8, 109.8, 101.4, 28.7, 25.2. FTIR (neat) cm^{-1}: 3179 (br-s), 2361 (w), 1702 (s), 1442 (m), 1205 (s), 1134 (s), 845 (m), 723 (m). HRMS (ESI, TOF) (*m*/*z*): calc'd for $C_{10}H_{17}N_6$, $[M+H]^+$: 221.1509, found: 221.1512.

1,8-Bis(5-benzyl-3-methyl-2-oxo-1,3,5-triazinan-1-yl)octane-2,7-dione (77)—Anhydrous tetrahydrofuran (8.0 mL, degassed thoroughly by passage of a stream of argon) was added via syringe to a flask charged with thioester **66** (70.9 mg, 0.198 mmol, 1 equiv), triazone **68** (290 mg, 0.494 mmol, 2.50 equiv), and copper(I)-thiophene-2-carboxylate (CuTC, 88.4 mg, 0.448 mmol, 2.25 equiv) at 23 °C under an argon atmosphere, and the reaction mixture was heated to 50 °C. After 1.5 h, the reaction mixture was allowed to cool to 23 °C. The resulting mixture was partitioned between dichloromethane (30 mL) and 5% ammonium hydroxide aqueous solution (30 mL). The aqueous layer was extracted with dichloromethane (30 mL), and the combined organic layers were dried over anhydrous sodium sulfate, were filtered, and were concentrated under reduced pressure. The crude residue was purified by flash column chromatography (silica gel: diam. 3 cm, ht. 11 cm; eluent: 24% chloroform, 5% methanol, and 0.6% ammonium hydroxide in dichloromethane) to afford ketotriazone **77** (89 mg, 82%) as a colorless oil. ^{1}H NMR (500 MHz, $CDCl_3$, 21 °C): δ 7.33–7.26 (m, 10H), 4.19 (s, 4H), 4.15 (s, 4H), 4.00 (s, 4H), 3.99 (s, 4H), 2.84 (s, 6H), 2.40 (t, *J* = 6.9 Hz, 4H), 1.57 (q, *J* = 3.3, 4H). ^{13}C NMR (100.6 MHz, $CDCl_3$, 21 °C): δ 206.9, 155.7, 137.8, 129.3, 128.8, 127.8, 67.8, 67.5, 55.6, 54.6, 39.6, 32.6, 23.0. FTIR (neat) cm^{-1}: 3442 (br-s), 2929 (m), 2237 (w), 1717 (m), 1635 (m), 1506 (m), 1266 (s), 739 (s). HRMS (ESI, TOF) (*m*/*z*): calc'd for $C_{30}H_{41}N_6O_4$, $[M+H]^+$: 549.3189, found: 549.3183. TLC (24% chloroform, 5.4% methanol, and 0.6% ammnoium hydroxide in dichloromethane), R*f*: 0.27 (CAM, UV).

Cell Culture Information

Cells were grown in media supplemented with fetal bovine serum (FBS) and antibiotics (100 μg/mL penicillin and 100 U/mL streptomycin). Specifically, experiments were performed using the following cell lines and media compositions: U-937, HeLa, A549, BT549, CEM, Daudi, and Jurkat (RPMI-1640 + 10% FBS), CA46 (DMEM + 10% FBS), HL-60 (IMDM + 10% FBS), and IMR90 (EMEM + 10% FBS). Cells were incubated at 37 °C in a 5% CO_2, 95% humidity atmosphere.

IC_{50} Value Determination for Adherent Cells using Sulforhodamine B (SRB)

Adherent cells (HeLa, A549, BT549, and IMR90) were added into 96-well plates (5,000 cells/well for HeLa cell line; 2,000 cells/well for A549, BT549, and IMR90 cell lines) in 100 μL media and were allowed to adhere for 2–3 hours. Compounds were solubilized in DMSO as 100x stocks, added directly to the cells (100 μL final volume), and tested over a range of concentrations (1 nM to 10 μM) in triplicate (1% DMSO final) on a half-log scale.

DMSO and cell-free wells served as the live and dead control, respectively. After 48 h of continuous exposure, the plates were evaluated using the SRB colorimetric assay as described previously.[62] Briefly, media was removed from the plate, and cells were fixed by the addition of 100 μL cold 10% trichloroacetic acid in water. After incubating at 4 °C for 1 h, the plates were washed in water and allowed to dry. Sulforhordamine B was added as a 0.057% solution in 1% acetic acid (100 μL), and the plates were incubated at room temperature for 30 min, washed in 1% acetic acid, and allowed to dry. The dye was solubilized by adding 10 mM Tris base solution (pH 10.5, 200 μL) and incubating at room temperature for 30 min. Plates were read at λ = 510 nm. IC_{50} values were determined from three or more independent experiments using TableCurve (San Jose, CA).

IC_{50} Value Determination for Non-Adherent Cells using MTS

In a 96-well plate, compounds were pre-added as DMSO stocks (1% final) in triplicate to achieve final concentrations of 1 nM to 10 μM on a half log scale. DMSO and cell-free wells served as the live and dead control, respectively. Suspension cells (U-937, CEM, CA46, Daudi, HL-60, and Jurkat; 10,000 cells/well) cells were distributed in 100 μL media to the compound-containing plate. After 48 h, cell viability was assessed by adding 20 μL of a PMS/MTS solution[63] to each well, allowing the dye to develop at 37 °C until the live control had processed MTS, and reading the absorbance at λ = 490 nm. IC_{50} values were determined from three or more independent experiments.

Hemolysis Assay using Human Erythrocytes

To prepare the erythrocytes, 0.1 mL of human blood was centrifuged (10,000 g, 2 min). The pellet was washed three times with saline (0.9% NaCl) via gentle resuspension and centrifugation (10,000 g, 2 min). Following the final wash, the erythrocytes were resuspended in 0.4 mL red blood cell (RBC) buffer (10 mM Na_2HPO_4, 150 mM NaCl, 1 mM $MgCl_2$, pH 7.4).

DMSO stocks of compounds were added to 0.5 mL tubes in singlicate (1 μL, 3.3% DMSO final). The stocks were diluted with 19 μL RBC buffer. Positive control tubes contained DMSO in water, and negative control tubes contained DMSO in RBC buffer. A suspension of washed erythrocytes (10 μL) was added to each tube, and samples were incubated at 37 °C for 2 hours. Samples were centrifuged (10,000 g, 2 min), and the supernatant was transferred to a clear, sterile 384-well plate. The absorbance of the supernatants was measured at λ = 540 nm, and percent hemolysis was calculated relative to the average absorbance values measured for the controls.

Apoptosis in U-937 Cells with Annexin V-FITC and Propidium Iodide (AnnV/PI)

DMSO stocks of compounds were added to a 24-well plate in singlicate (0.2% DMSO final). After compound addition, 0.5 mL of a U-937 cell suspension (250,000 cells/mL) was added and allowed to incubate for 21 hours. Following treatment, the cell suspensions were transferred to flow cytometry tubes and pelleted (500 g, 3 min). The media was removed by aspiration, and cells were resuspended in 200 μL AnnV binding buffer (10 mM HEPES, pH 7.4, 140 mM NaCl, 2.5 mM $CaCl_2$) with 5 μg/mL PI and 1:90 dilution of AnnV. Samples were analyzed using flow cytometry.

Cell Cycle Arrest in Thymidine-Synchronized U-937 Cells

U-937 cells were split to 50% confluency (250,000 cells/mL) and treated with 2 mM thymidine for 10 hours. The cells were then pelleted (500 g, 3 minutes) and washed with PBS before being resuspended in thymidine-free media and allowed to recover for 13 hours.

The cells were then re-blocked with 2 mM thymidine for 10 hours, and then washed with PBS as before and resuspended in media (250,000 cells/mL).

DMSO stocks of compounds were added to a 24-well plate in triplicate (0.2% DMSO final), after which 1 mL of the prepared cell suspension was added. Following a 16 h incubation, the cell suspensions were transferred to 2 mL tubes and pelleted (600 g, 3 min). The media was removed by aspiration, and the cells were fixed with 0.5 mL of ice cold 70% ethanol with vortexing. The samples were fully fixed at −20 °C for 3 hours. The samples were then pelleted (1000 g, 5 min) and the supernatant was removed via aspiration. The cells were incubated with 50 μL of 5 μg/mL RNAseA in PBS for 3 hours at room temperature. Prior to reading, the samples were taken up in 150 μL of 50 μg/mL propidium iodide in PBS and transferred to flow cytometry tubes. Samples were analyzed based on whole, single cells.

Tubulin Microscopy with HeLa Cells

Round, 1.5 mm coverslips (No. 1.5) were sterilized with ultraviolet light and placed in a 12-well plate. HeLa cells (100,000 cells/well) were added and allowed to adhere for eight hours. Compounds were then added as DMSO stocks to achieve a final DMSO concentration of 1%, and the plates were returned to the incubator for 16 hours.

Following incubation, the media was removed, and the coverslips were fixed with 0.5 mL Microtubulin Stabilizing Buffer (MTSB, 80 mM PIPES, pH 6.8, 1 mM $MgCl_2$, 5 mM EGTA, 0.5% TX-100) + 0.5% glutaraldehyde for 10 minutes at room temperature, after which the fixative was removed and the sample was quenched with the addition of 0.5 mL of freshly-prepared 1 mg/mL $NaBH_4$ in PBS. After a 5 min incubation, the solution was removed by aspiration and the coverslips were washed with PBS.

Coverslips were transferred to parafilm-lined culture dishes (cell-side up), and 40 μL of 50 μg/mL RNase A in Antibody Diluting Solution (AbDil, PBS, pH 7.4, 0.2% TX-100, 2% BSA, 0.1% NaN_3) with 1:50 dilution of anti-α-tubulin-FITC antibody was added to all samples. The samples were allowed to incubate at room temperature in the dark for 2.5 hours, after which the coverslips were washed three times with PBS + 0.1% TX-100. The samples were then incubated for 2 minutes with 50 μL of 50 μg/mL PI in PBS. The coverslips were washed three times with PBS + 0.1% TX-100, at which point they were mounted onto microscopy slides, allowed to cure, and imaged.

Supplementary Material

Refer to Web version on PubMed Central for supplementary material.

Acknowledgments

We acknowledge financial support by NIH-NIGMS (GM074825) and the University of Illinois. We thank Dr. Justin Kim, and Dr. Peter Müller for assistance with X-ray crystallographic analysis. We thank Dr. Stephen Lathrop for preparation of new samples for biological study. K.C.M. is a National Science Foundation predoctoral fellow and a Robert C. and Carolyn J. Springborn graduate fellow.

References and Footnotes

1. (a) D’Ambrosio M, Guerriero A, Debitus C, Ribes O, Pusset J, Leroy S, Pietra F. J Chem Soc, Chem Commun. 1993:1305.(b) D’Ambrosio M, Guerriero A, Chiasera G, Pietra F. Helv Chim Acta. 1994; 7:1895.(c) D’Ambrosio M, Guerriero A, Ripamonti M, Debitus C, Waikedre J, Pietra F. Helv Chim Acta. 1996; 79:727.
2. Pettit GR, Ducki S, Herald DL, Doubek DL, Schmidt JM, Chapuis J. Oncol Res. 2005; 15:11. [PubMed: 15839302]

3. Hong TW, Jímenez DR, Molinski TF. J Nat Prod. 1998; 61:158. [PubMed: 9461668]
4. Tilvi S, Moriou C, Martin M, Gallard J, Sorres J, Patel K, Petek S, Debitus C, Ermolenko L, Al-Mourabit A. J Nat Prod. 2010; 73:720. [PubMed: 20166736]
5. Hale, KJ.; Domostoj, MM.; El-Tanani, M.; Campbell, FC.; Mason, CK. Strategies and Tactics in Organic Synthesis. Harmata, M., editor. Vol. 6. Elsevier Academic Press; London: 2005. p. 352-394.ch. 11
6. Li Z, Shigeoka D, Caulfield TR, Kawachi T, Qiu Y, Kamon T, Arai M, Tun HW, Yoshimitsu T. Med Chem Commun. 2013; 4:1093.
7. Mason CK, McFarlane S, Johnston PG, Crowe P, Erwin PJ, Domostoj MM, Campbell FC, Manaviazar S, Hale KJ, El-Tanani M. Mol Cancer Ther. 2008; 7:548. [PubMed: 18347142]
8. Li Z, Kamon T, Personett DA, Caulfield T, Copland JA, Yoshimitsu T, Tun HW. Med Chem Comm. 2012; 3:233.
9. Meijer L, Thunnissen A, White AW, Garnier M, Nikolic M, Tsai L, Walter J, Cleverley KE, Salinas PC, Wu Y, Biernat J, Mandelkow E, Kim S, Pettit GR. Chem Biol. 2000; 7:51. [PubMed: 10662688]
10. Morales JJ, Rodriguez AD. J Nat Prod. 1991; 54:629.
11. Kobayashi J, Ohizumi H, Hirata Y. Experientia. 1986; 42:1176. [PubMed: 3770140]
12. Forenza S, Minale L, Riccio R, Fattorusso E. J Chem Soc, Chem Commun. 1971:1129.
13. Garcia EE, Benjamin LE, Fryer RI. J Chem Soc, Chem Commun. 1973:78.
14. Andrade P, Willoughby R, Pomponi SA, Kerr RG. Tetrahedron Lett. 1999; 40:4775.
15. For an informative enzymatic conversion of oroidin into benzosceptrin C and nagelamide H, see: Stout EP, Wang YG, Romo D, Molinski TF. Angew Chem Int Ed. 2012; 51:4877.
16. Movassaghi M, Siegel DS, Han S. Chem Sci. 2010; 1:561. [PubMed: 21218186]
17. (a) Al-Mourabit A, Potier P. Eur J Org Chem. 2001:237.(b) Al-Mourabit A, Zancanella MA, Tilvi S, Romo D. Nat Prod Rep. 2011; 28:1229. [PubMed: 21556392]
18. For a review on total synthesis of agelastatin alkaloids, see: Dong G. Pure Appl Chem. 2010; 82:2231.
19. For the total synthesis of agelastatin alkaloid, see: Stien D, Anderson GT, Chase CE, Koh Y, Weinreb SM. J Am Chem Soc. 1999; 121:9574.Feldman KS, Saunders JC. J Am Chem Soc. 2002; 124:9060. [PubMed: 12149004] Feldman KS, Saunders JC, Wrobleski ML. J Org Chem. 2002; 67:7096. [PubMed: 12354005] Domostoj MM, Irving E, Scheinmann F, Hale KJ. Org Lett. 2004; 6:2615. [PubMed: 15255704] Davis FA, Deng J. Org Lett. 2005; 7:621. [PubMed: 15704909] Trost BM, Dong G. J Am Chem Soc. 2006; 128:6054. [PubMed: 16669672] Ichikawa Y, Yamaoka T, Nakano K, Kotsuki H. Org Lett. 2007; 9:2989. [PubMed: 17602639] Yoshimitsu T, Ino T, Tanaka T. Org Lett. 2008; 10:5457. [PubMed: 19006318] Dickson PD, Wardrop DJ. Org Lett. 2009; 11:1341. [PubMed: 19228041] Hama N, Matsuda T, Sato T, Chida N. Org Lett. 2009; 11:2687. [PubMed: 19449885] When PM, Du Bois J. Angew Chem, Int Ed Engl. 2009; 48:3802. [PubMed: 19378315] Davis FA, Zhang Y, Qiu H. Synth Comm. 2009; 39:1914.Trost BM, Dong G. Chem-Eur J. 2009; 15:6910. [PubMed: 19533707] For the formal total synthesis of agelastatin alkaloid, see: Hale KJ, Domostoj MM, Tocher DA, Irving E, Scheinmann F. Org Lett. 2003; 5:2927. [PubMed: 12889910] Yoshimitsu T, Ino T, Futamura N, Kamon T, Tanaka T. Org Lett. 2009; 11:3402. [PubMed: 19588910] For the synthetic studies toward the agelastatin alkaloid, see: Anderson GT, Chase CE, Koh Y, Stien D, Weinreb SM. J Org Chem. 1998; 63:7594.Baron E, O'Brien P, Towers TD. Tetrahedron Lett. 2002; 43:723.Porter MJ, White NJ, Howells GE, Laffan DDP. Tetrahedron Lett. 2004; 45:6541.
20. For the recent total synthesis of agelastatin A (**1**), see: Kano T, Sakamoto R, Akakura M, Maruoka K. J Am Chem Soc. 2012; 134:7516. [PubMed: 22486203] Reyes JP, Romo D. Angew Chem Int Ed. 2012; 51:6870.For the recent formal total synthesis of agelastatin A (**1**), see: Menjo Y, Hamajima A, Sasaki N, Hamada Y. Org Lett. 2011; 13:5744. [PubMed: 21966984] Shigeoka D, Kamon T, Yoshimitsu T. Beilstein, J Org Chem. 2013; 9:860. [PubMed: 23766801]
21. For an acid promoted conversion of oroidin to (±)-cyclooroidin (**11**), see: Pöverlein C, Breckle G, Lindel T. Org Lett. 2006; 8:819. [PubMed: 16494449]
22. (a) Poullennec KG, Romo D. J Am Chem Soc. 2003; 125:6344. [PubMed: 12785755] (b) Hasse K, Willis AC, Banwell MG. Aus J Chem. 2009; 62:683.

23. Narayana Murthy S, Nageswar YVD. Tetrahedron Lett. 2011; 52:4481.
24. Oussaid B, Garrigues B, Souflaoui M. Can J Chem. 1994; 72:2483.
25. Kurosawa W, Kan T, Fukuyama T. J Am Chem Soc. 2003; 125:8112. [PubMed: 12837075]
26. Han S, Siegel DS, Movassaghi M. Tetrahedron Lett. 2012; 53:3722. [PubMed: 22844161]
27. For a recent review, see: Campos KR. Chem Soc Rev. 2007; 36:1069. [PubMed: 17576475]
28. For related examples, see: Shono T, Matsumura Y, Tsubata K. J Am Chem Soc. 1981; 103:1172.Sud A, Sureshkumar D, Klussmann M. Chem Comm. 2009:3169. [PubMed: 19587902] McNally A, Prier CK, MacMillan DWC. Science. 2011; 334:1114. [PubMed: 22116882]
29. For representative examples, see: Shono T, Matsumura Y, Uchida K, Kobayashi H. J Org Chem. 1985; 50:3243.Lennartz M, Sadakane M, Steckhan E. Tetrahedron. 1999; 55:14407.Izawa K, Nishi S, Asada S. J Mol Cat. 1987; 41:135.Murahashi SI, Naota T, Kuwabara T, Saito T, Kumobayashi H, Akutagawa S. J Am Chem Soc. 1990; 112:7820.Murahashi SI, Saito T, Naota T, Kumobayashi H, Akutagawa S. Tetrahedron Lett. 1991; 32:2145.Murahashi SI, Saito T, Naota T, Kumobayashi H, Akutagawa S. Tetrahedron Lett. 1991; 32:5991.Naota T, Nakato T, Murahashi SI. Tetrahedron Lett. 1990; 31:7475.Shirakawa E, Uchiyama N, Hayashi T. J Org Chem. 2011; 76:25. [PubMed: 21158393] For a review on synthetic applications of anodic electrochemistry, see: Moeller KD. Tetrahedron. 2000; 56:9527.
30. Mukaiyama T, Matsuo J-i, Yanagisawa M. Chem Lett. 2000:1072.
31. We also examined the use of self-oxidizing protective groups at N9 of lactam **18**. However, we could not confirm the formation of acylimine **19**. For related methodology, see: Curran DP, Yu H. Synthesis. 1992; 123
32. Negoro T, Murata M, Ueda S, Fujitani B, Ono Y, Kuromiya A, Komiya M, Suzuki K, Matsumoto J. J Med Chem. 1998; 41:4118. [PubMed: 9767647]
33. We advanced the racemic samples of imides **25a** and **25b** for prompt assessment of our planned C4–C8 bond formation and acquisition of intermediates, in racemic form, as reference for synthesis of (−)-**1**.
34. (a) Hassel T, Seebach D. Helv Chim Acta. 1978; 61:2237.(b) Beak P, Zajdel WJ, Reitz DB. Chem Rev. 1984; 84:471.(c) Pearson WH, Lindbeck AC, Kampf JW. J Am Chem Soc. 1993; 115:2622.
35. (a) Marckwald W. Chem Ber. 1892; 25:2354.(b) Duschinsky R, Dolan LA. J Am Chem Soc. 1946; 68:2350. [PubMed: 21002238]
36. Pyrrolopyrazinone **36** was the major product formed under various acidic reaction conditions examined for this transformation.
37. See the supporting information for details.
38. Nakamura S, Hirao H, Ohwada T. J Org Chem. 2004; 69:4309. [PubMed: 15202884]
39. This 5-(enolendo)-exo-trig type of cyclization with an acyliminium ion is a rare and challenging transformation consistent with the paucity of reported cases. For examples of this type of cyclization, see: Gramain JC, Remuson R. Heterocycles. 1989; 29:1263.Heaney H, Taha MO. Tetrahedron Lett. 1998; 39:3341.
40. We observed 67% conversion of (+)-**41** to B-ring cyclized product within five minutes.
41. (a) Wittenberg R, Srogl J, Egi M, Liebeskind LS. Org Lett. 2003; 5:3033. [PubMed: 12916974] (b) Li H, Yang H, Liebeskind LS. Org Lett. 2008; 10:4375. [PubMed: 18759432] (c) Zhang Z, Lindale MG, Liebeskind LS. J Am Chem Soc. 2011; 133:6403. [PubMed: 21449537] (d) Li H, He A, Falck JR, Liebeskind LS. Org Lett. 2011; 13:3682. [PubMed: 21675755]
42. For a review on palladium-mediated synthesis of aldehydes and ketones from thioester, see: Fukuyama T, Tokuyama H. Aldrichchimica Acta. 2004; 37:87.
43. (a) Falck JR, Bhatt RK, Ye J. J Am Chem Soc. 1995; 117:5973.(b) Lange H, FrÖhlich R, Hoppe D. Tetrahedron. 2008; 64:9123.
44. (a) Labadie JW, Tueting D, Stille JK. J Org Chem. 1983; 48:4634.(b) Yasuda N, Yang C, Wells KM, Jensen MS. Tetrahedron Lett. 1990; 40:427.(c) Ferezou JP, Julia M, Li Y, Liu LW, Pancrazi A. Synlett. 1991:53.
45. (a) Vedejs E, Haight AR, Moss WO. J Am Chem Soc. 1992; 114:6556.(b) Jensen MS, Yang C, Hsiao Y, Rivera N, Wells KM, Chung JYL, Yasuda N, Hughes DL, Reider PJ. Org Lett. 2000; 2:1081. [PubMed: 10804559]

46. Linderman RJ, Siedlecki JM. J Org Chem. 1996; 61:6492. [PubMed: 11667508]
47. This observation is consistent with reaching a thermodynamic ratio of **1** and **40** (Scheme 8) under these reaction conditions.
48. For a prior semi-synthesis of (−)-**51** from (−)-**5**, see ref 1c. Notably, we observed that (−)-**50** underwent loss of methanol faster than (−)-**5**.
49. We attribute the low yield of this transformation to the sensitivity of tetracycle **56**.
50. Neither the optical rotation nor the ^{13}C NMR spectrum of agelastatin D (**4**) was obtained in the original isolation report (ref 3) as it was a minor component.
51. Koswatta PB, Lovely CJ. Nat Prod Rep. 2011; 28:511. [PubMed: 20981389]
52. Notably, the observed selectivity of (−)-agelastatin A (**1**) for blood cancers is unusual and distinguishes it from other bioactive natural products. For a recent report on challenges regarding the selectivity to cancer subpopulations, see: Basu A, Bodycombe NE, Cheah JH, Price EV, Liu K, Schaefer GI, Ebright RY, Stewart ML, Ito D, Wang S, Bracha AL, Liefeld T, Wawer M, Gilbert JC, Wilson AJ, Stransky N, Kryukov GV, Dancik V, Barretina J, Garraway LA, Hon S, Munoz B, Bittker JA, Stockwell BR, Khabele D, Stern AM, Clemons PA, Shamji AF, Schreiber SL. Cell. 2013; 154:1151. [PubMed: 23993102]
53. Chan WI, Huntly BJP. Semin Oncol. 2008; 35:326. [PubMed: 18692683]
54. Kepp O, Galluzzi L, Lipinski M, Yuan J, Kroemer G. Nature Rev Drug Disc. 2011; 10:221.
55. (a) Hanahan D, Weinberg RA. Cell. 2000; 100:57. [PubMed: 10647931] (b) Hanahan D, Weinberg RA. Cell. 2011; 144:646. [PubMed: 21376230]
56. Krysko D, Vanden Berghe T, D'Herde K, Vandenabeele P. Methods. 2008; 44:205. [PubMed: 18314051]
57. For examples of using high concentration (>100-fold over IC_{50}) of taxol in experiments evaluating tubulin polymerization, see: Saxton WM, Stemple DL, Leslie RJ, Salmon ED, Zavortink M, Mcintosh R. J Cell Biol. 1984; 99:2175. [PubMed: 6501419] Wilson L, Panda D, Jordan MA. Cell Struct Funct. 1999; 24:329. [PubMed: 15216890] Matsuyama A, Shimazu T, Sumida Y, Saito A, Yoshimatsu Y, Seigneurin-Bermy D, Osada H, Komatsu Y, Nishino N, Khochbin S, Yoshida M. EMBO J. 2002; 21:6820. [PubMed: 12486003] Shannon KB, Canman JC, Moree CB, Tirnauer JS, Salmon ED. Mol Biol Cell. 2005; 16:4423. [PubMed: 15975912] Hornick JE, Bader JR, Tribble EK, Trimble K, Breunig JS, Halpin ES, Vaughan KT, Hinchcliffe EH. Cell Motil Cytoskeleton. 2008; 65:595. [PubMed: 18481305]
58. (a) Bhalla KN. Oncogene. 2003; 22:9075. [PubMed: 14663486] (b) Dumontet C, Sikic BI. J Clin Oncol. 1999; 17:1061. [PubMed: 10071301]
59. See Figure S4 in the supporting information.
60. Lees WJ, Singh R, Whitesides GM. J Org Chem. 1991; 56:7328.
61. The use of organostannane **46** in place of **47** afforded ketotriazone **72** in 52% yield.
62. Vichai V, Kirtikara K. Nature Prot. 2006; 1:1112.
63. Cory AH, Owen TC, Barltrop JA, Cory JG. Cancer Commun. 1991; 3:207. [PubMed: 1867954]

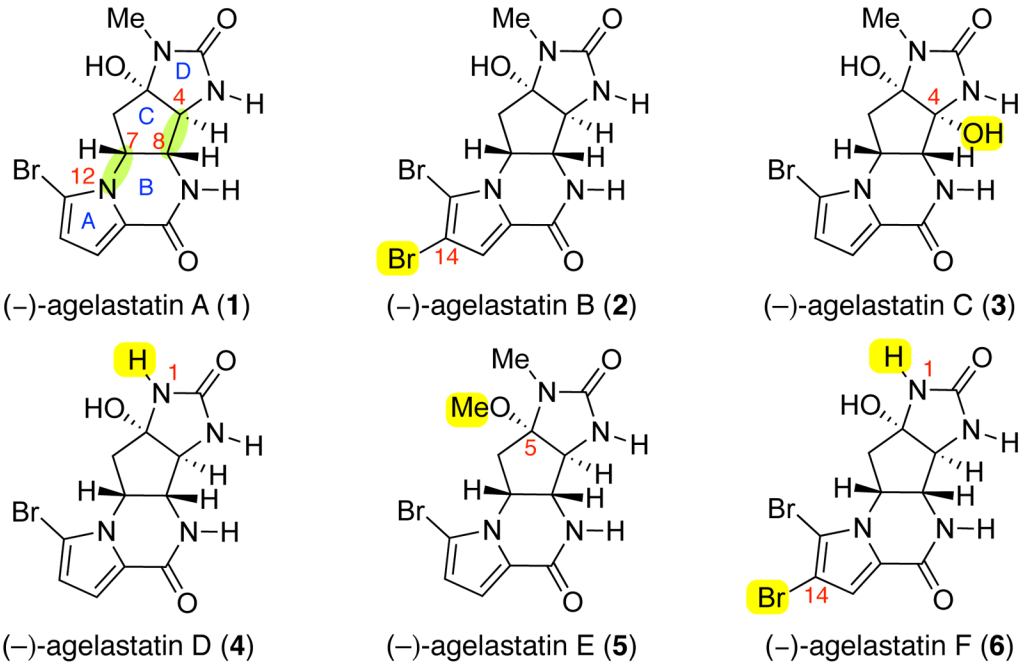

Figure 1.
The structures of (−)-agelastatins A–F (**1**–**6**).

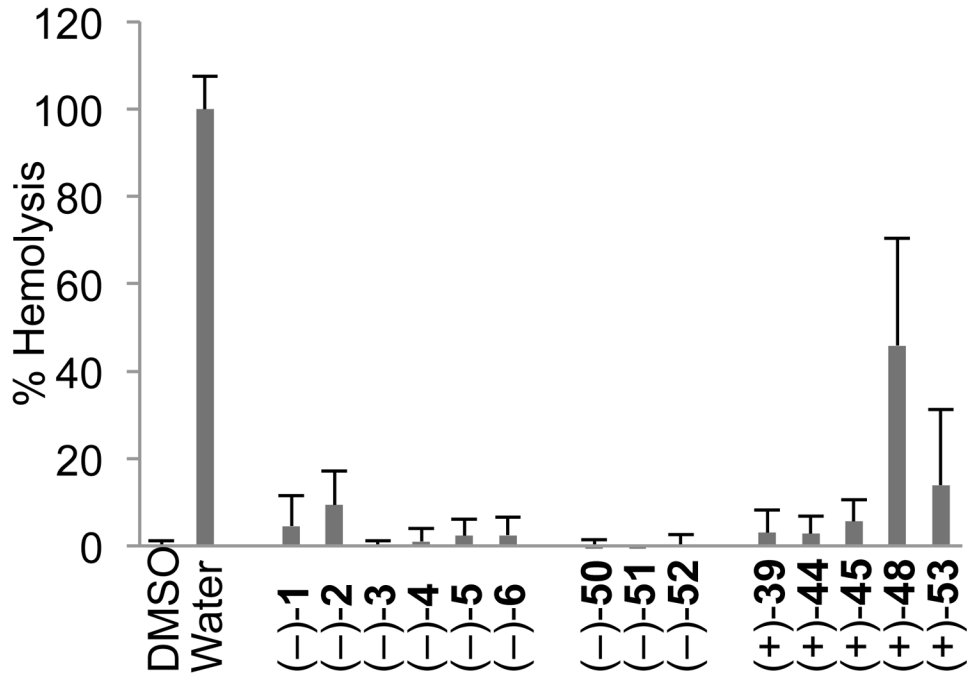

Figure 2.

Hemolytic activity of (−)-agelastatins A–F and advanced intermediates. Compounds were tested at 333 μM and hemolysis was evaluated after 2 h. DMSO and water served as the negative and positive controls for hemolysis, respectively. Error bars represent standard deviation of the mean, $n = 3$.

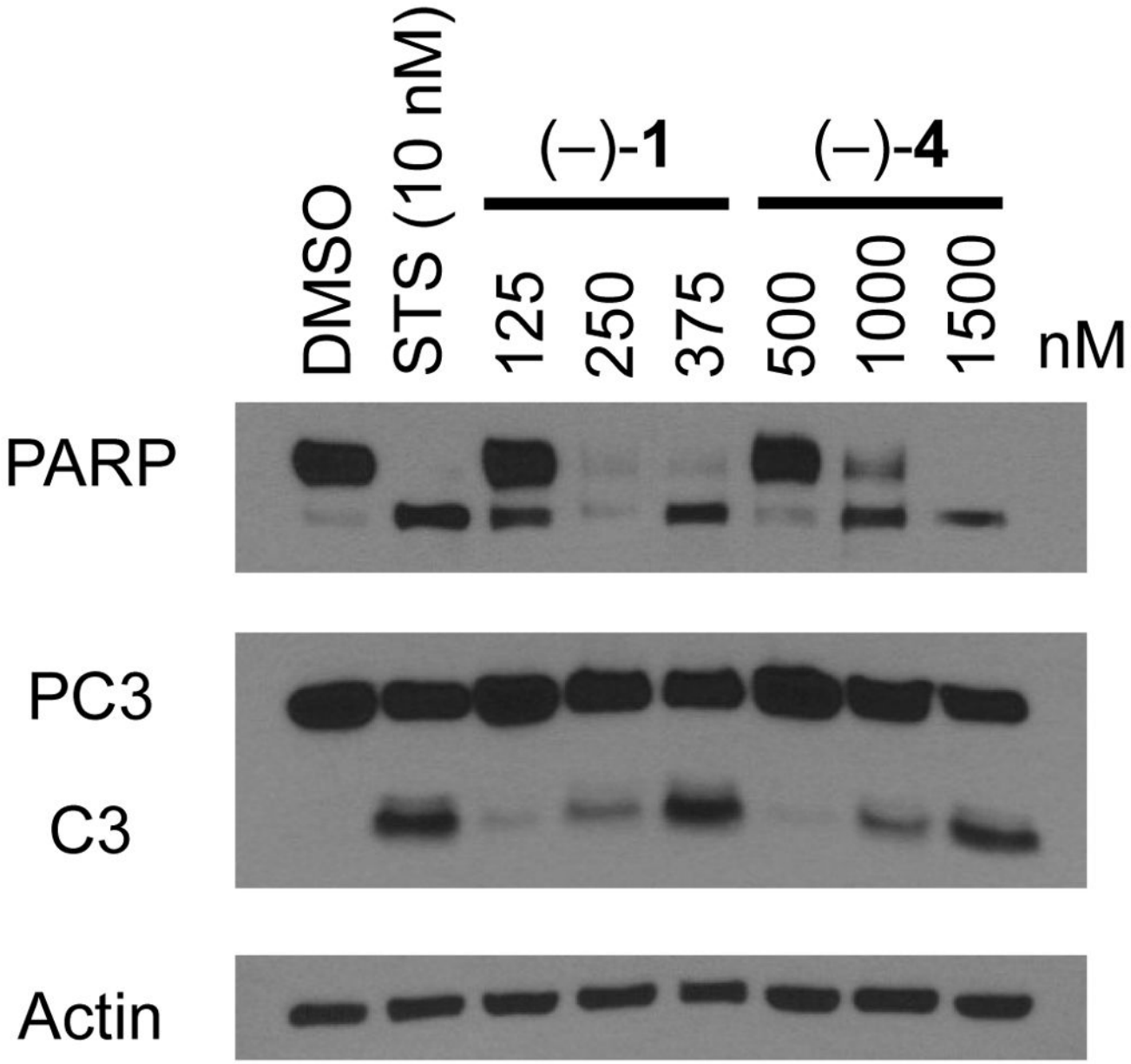

Figure 3.

(−)-Agelastatins A (**1**) and D (**4**) both induce caspase-dependent apoptotic cell death. Western blot analysis of procaspase-3 and PARP-1 cleavage at 24 hours in U-937 cells using β-actin as loading control. Compounds were tested at indicated concentrations (twice, four times, and six times the 48-hour IC_{50} value) and STS (10 nM); C3 = caspase-3; PARP = poly(ADP-ribose) polymerase 1; PC3 = procaspase-3; STS = staurosporine.

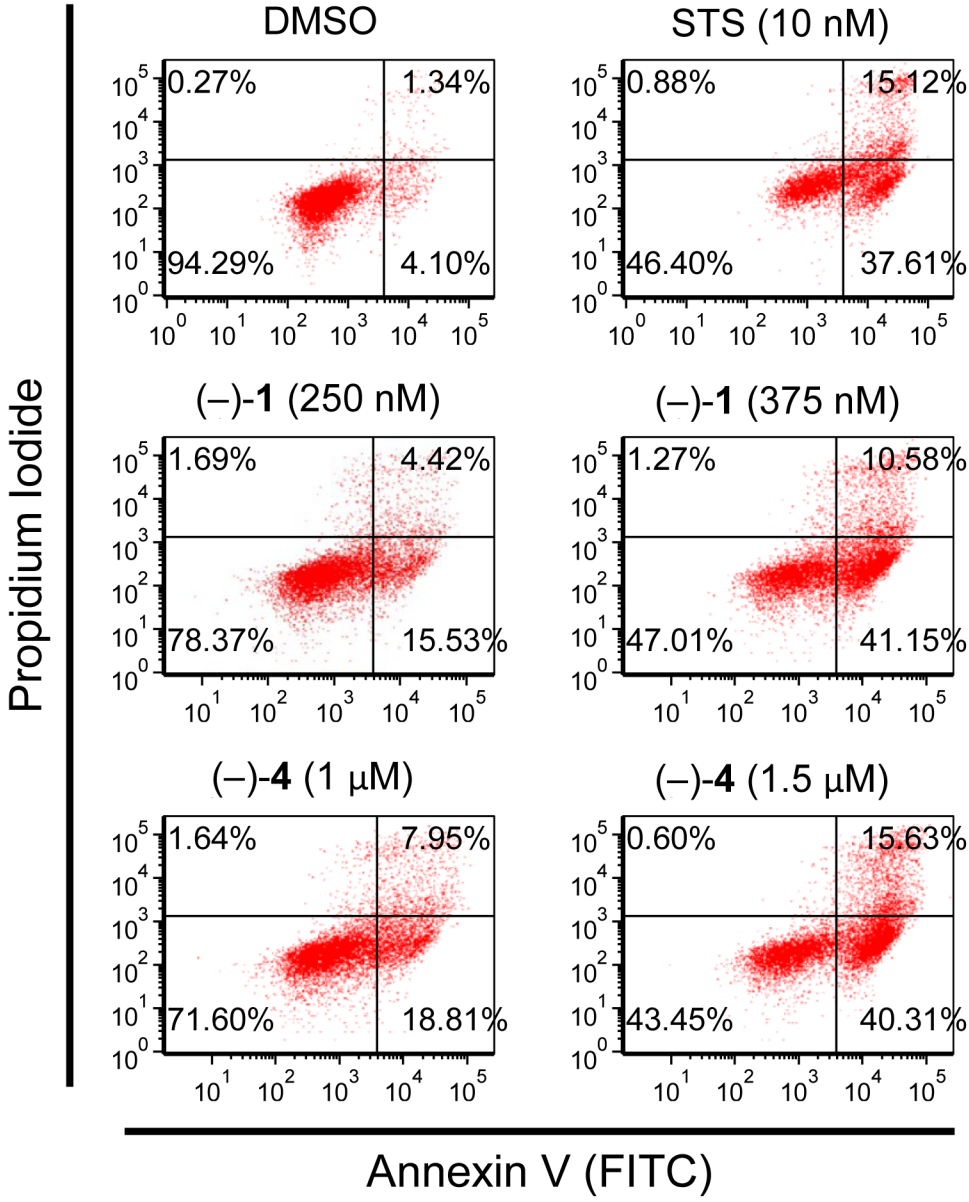

Figure 4.

(−)-Agelastatins A (**1**) and D (**4**) both induced dose-dependent apoptosis. Analysis of phosphatidylserine exposure and propidium iodide inclusion at 21 hours in U-937 cells. Compounds were tested at indicated concentrations (four and six times the 48-hour IC_{50} value) and STS was used as a positive control for apoptosis. Samples were analyzed by flow cytometry for the relative timing of phosphatidylserine exposure relative to PI inclusion. FITC = fluorescein isothiocyanate; PI = propidium iodide; STS = staurosporine.

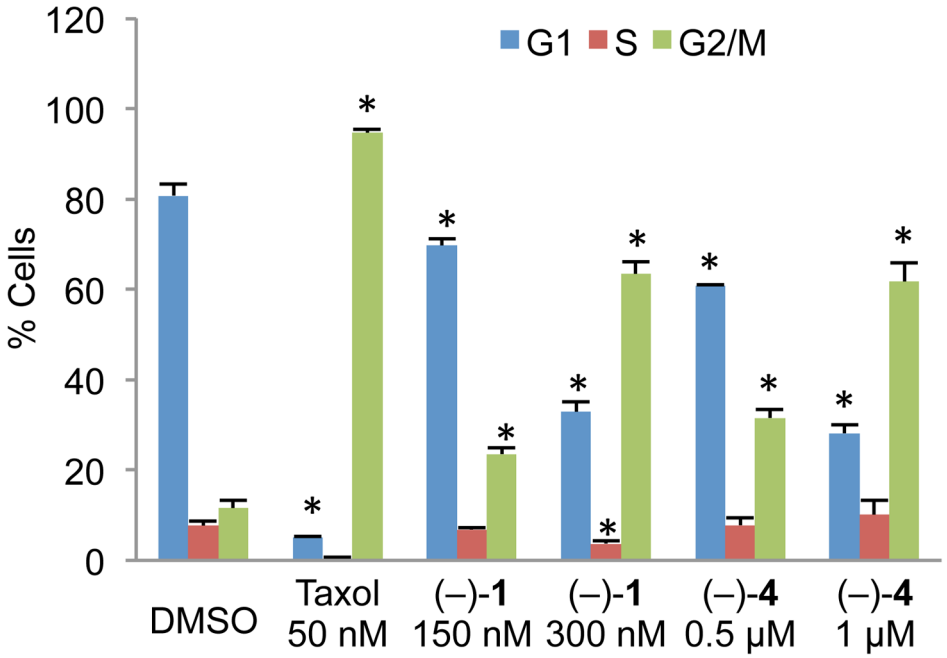

Figure 5.

(−)-Agelastatins A (**1**) and D (**4**) both exhibit dose-dependent G2/M cell cycle arrest in synchronized U-937 cells after 16 hours. Samples were fixed, treated with a RNAse, stained with PI, and analyzed by flow cytometry. Taxol, a microtubule stabilizer, was used as a positive control. Error bars represent standard deviation of the mean, n=3. * $p<0.01$. PI = propidium iodide.

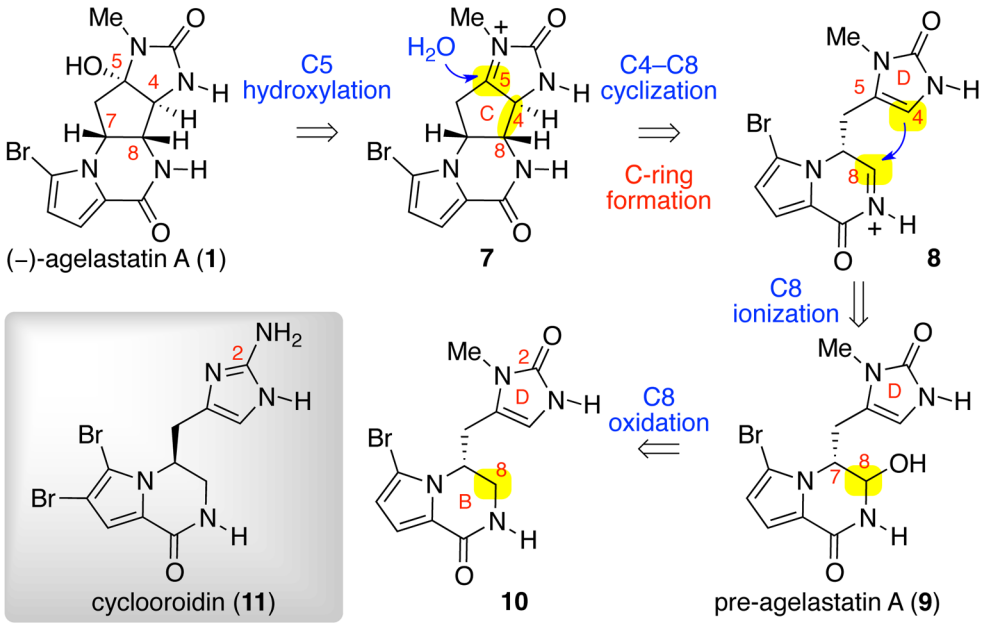

Scheme 1.
Retrobiosynthetic analysis of (−)-agelastatin A (**1**).

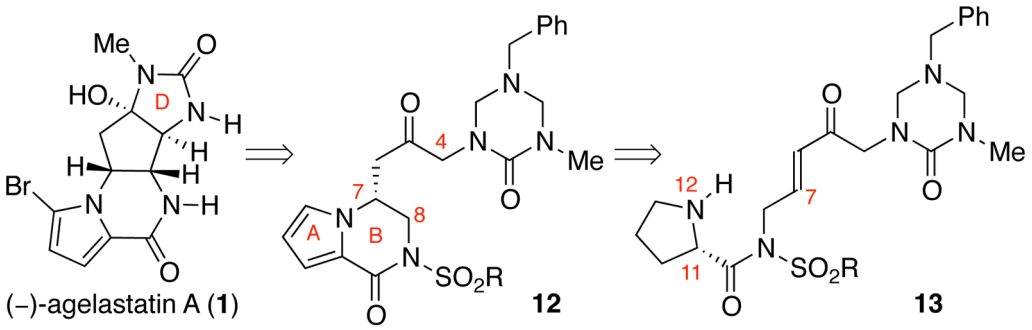

Scheme 2.
An early approach toward (−)-agelastatin A (**1**).

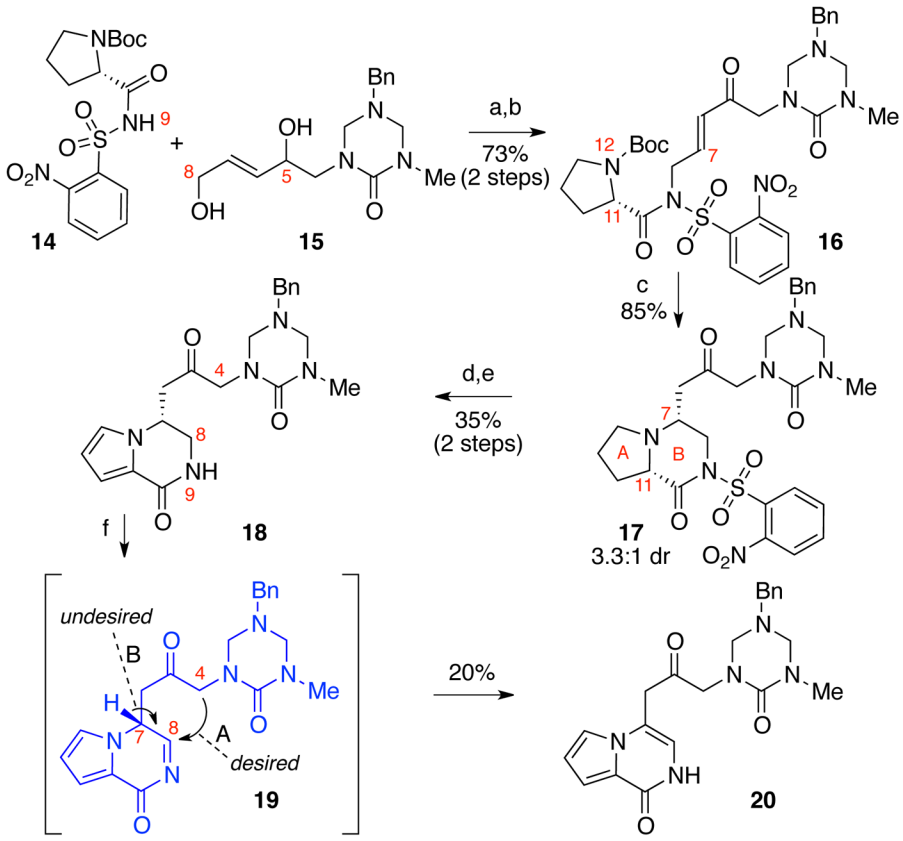

Scheme 3.

Synthesis of key bicycle **18** and attempted oxidation–cyclization. Conditions: (a) DEAD, PPh_3, THF, 0→23 °C, 79%; (b) DMP, CH_2Cl_2, 23 °C, 93%; (c) TFA, CH_2Cl_2, 0 °C, 85%; (d) DMP, CH_2Cl_2, 23 °C, 42%; (e) PhSH, KOH, MeCN, 0 °C, 84%; (f) *N*-*t*-butylbenzenesulfinimidoyl chloride, DBU, CH_2Cl_2, −78→23 °C, 20%; DEAD = diethyl azodicarboxylate, DBU = 1,8-diazabicycloundec-7-ene.

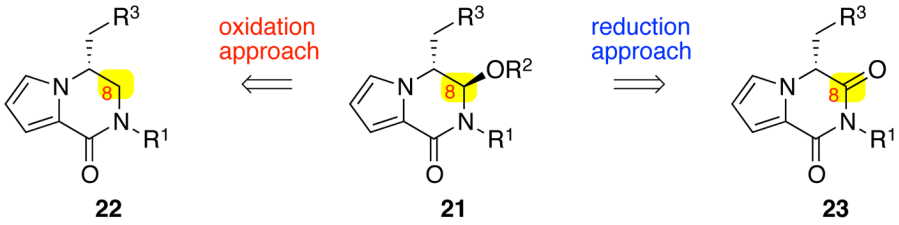

Scheme 4.
Two strategies for the introduction of the C8-hemiaminal ether **21**.

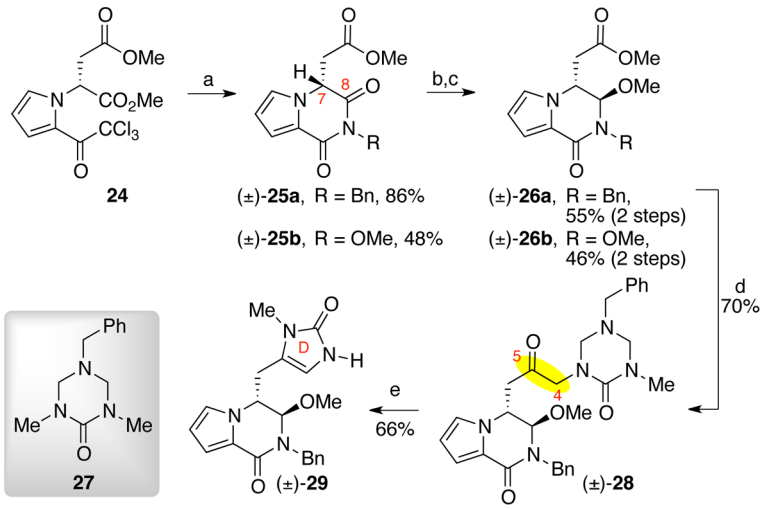

Scheme 5.

Synthesis of imidazolone (±)-**29**. Conditions: (a) H_2NR, DMF, 23 °C (R=Bn: 86%, R=OMe: 48%); (b) L-selectride, −78 °C, THF (R=Bn: 78%, R=OMe: 58%); (c) TsOH•H_2O, MeOH, 23 °C (R=Bn: 70%, R=OMe: 95%); (d) **27**, *s*-BuLi, TMEDA, THF, −78 °C, 70%; (e) HCl (aq.), MeOH, 23 °C, 66%, TsOH = *p*-toluenesulfonic acid.

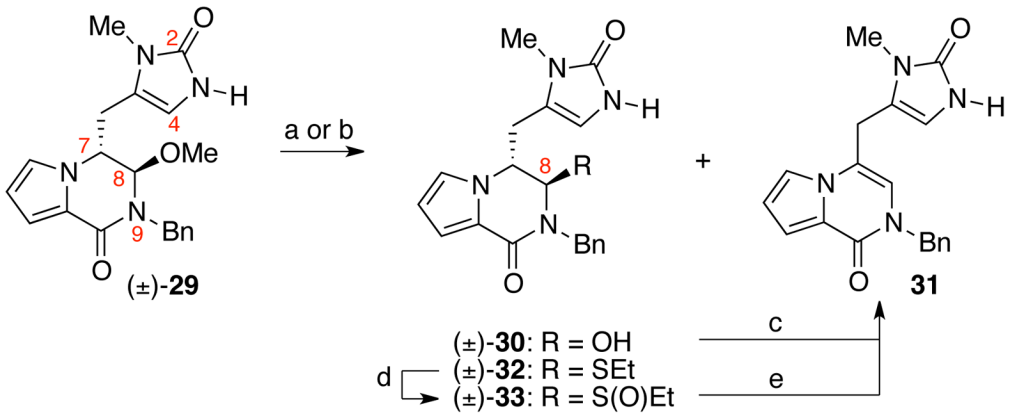

Scheme 6.

Formation of pyrrolopyrazinone **31** under various conditions. Conditions: (a) $Sc(OTf)_3$, H_2O, CH_3CN, 23 °C [(±)-**30:** 36%, **31**: <5%]; (b) EtSH, TFA, CH_2Cl_2, 23 °C [(±)-**32**: 95%]; (c) CH_2Cl_2, TFA, 23 °C, 95%; (d) $NaIO_4$, MeOH, H_2O, 23 °C, 55%; (e) MeCN, 79 °C, 100 %.

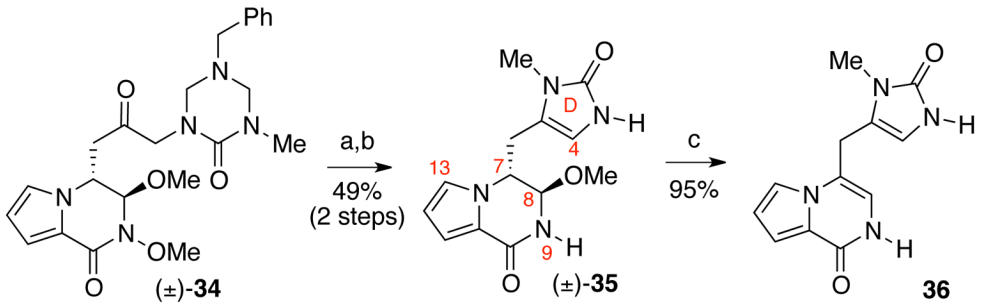

Scheme 7.

Synthesis of imidazolone derivative (±)-**35** and its reactivity under acidic condition. Conditions: (a) SmI_2, THF, MeOH, −78 °C, 73%; (b) HCl (aq.), MeOH, 23 °C, 67%; (c) TFA, H_2O, MeCN, 23 °C, 95%.

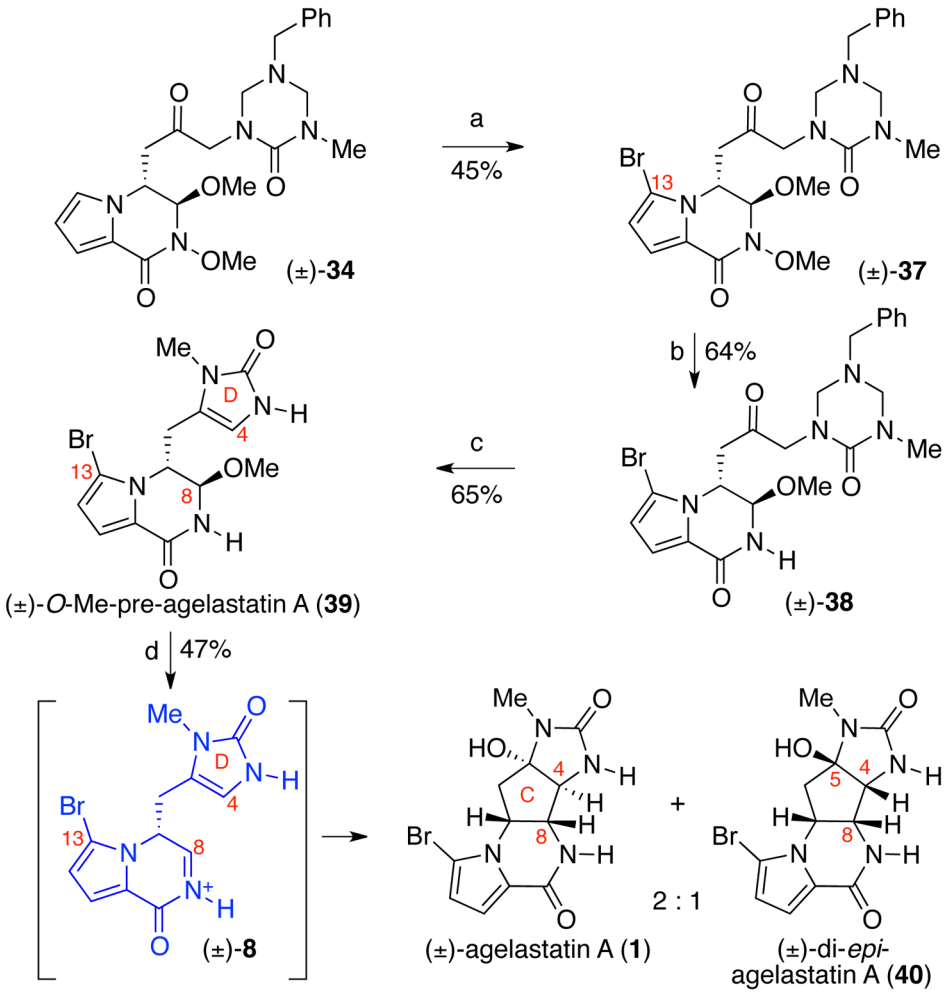

Scheme 8.

Our first generation total synthesis of (±)-agelastatin A (**1**). Conditions: (a) NBS, MeCN, 0 °C, 45%; (b) SmI_2, THF, −78 °C, 64%; (c) HCl (aq.), MeOH, 23 °C, 65%; (d) H_2O, MeCN, TFA, 40 °C, 47% (2: 1, (±)-**1**: (±)-**40**); NBS = *N*-bromosuccinimide.

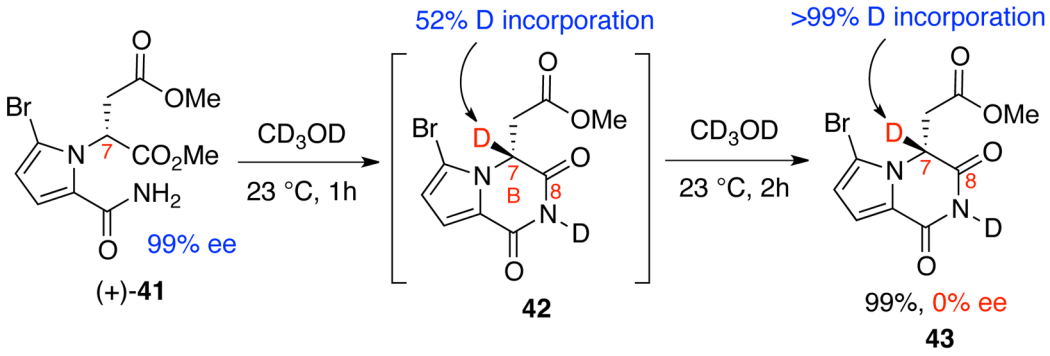

Scheme 9.
Cyclization and deuterium incorporation at C7 of amide (+)-**41**.

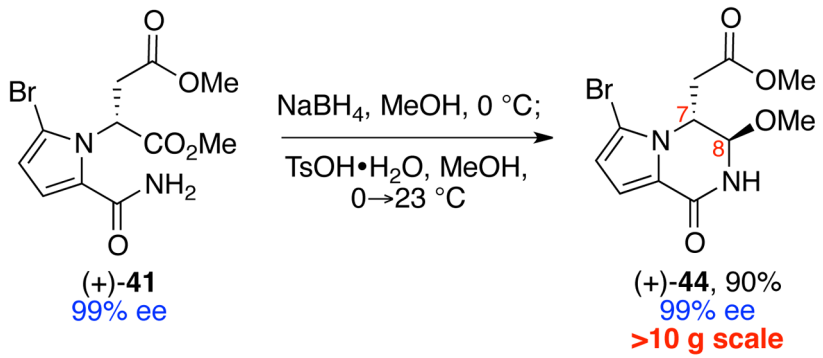

Scheme 10.
Synthesis of bicycle (+)-**44**.

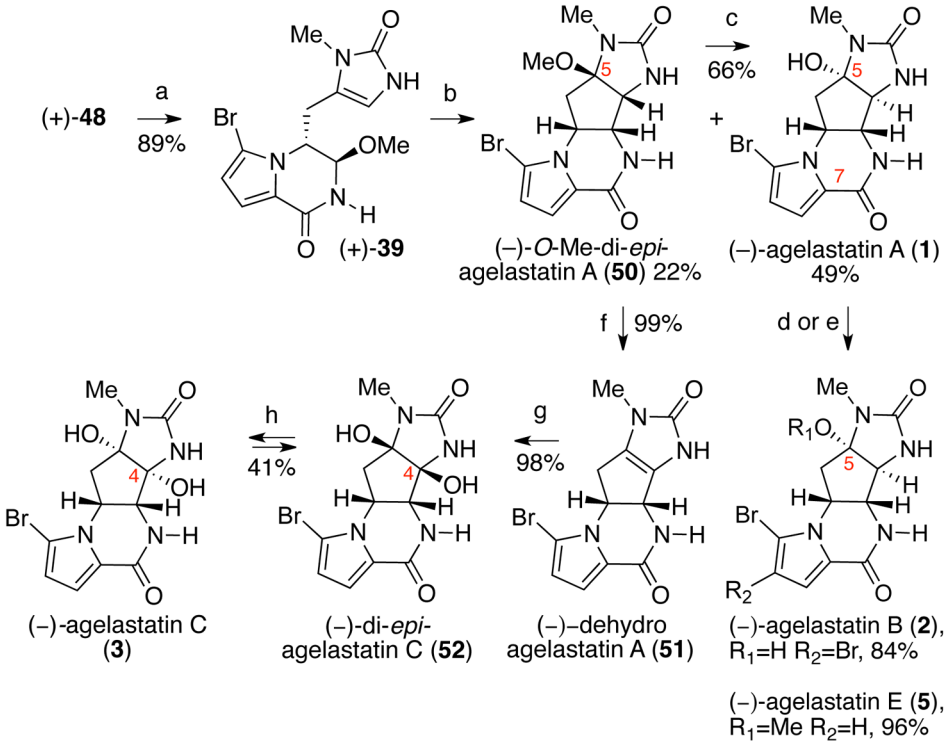

Scheme 11.

Enantioselective synthesis of (−)-agelastatins A–C (**1**–**3**) and E (**5**). Conditions: (a) HCl (aq.), MeOH, 65 °C, 89%; (b) $MeSO_3H$, H_2O, 100 °C; MeOH, 71% [2:1, (−)-**1**:(−)-**50**]; (c) $MeSO_3H$, H_2O, 100 °C; MeOH [66% of (−)-**1**, and 30% of recovered (−)-**50**]; (d) NBS, DTBMP, THF, H_2O, 0 °C, 84% (**1**→**2**); (e) Amberlyst 15, MeOH, 65 °C, 96% (**1**→**5**); (f) pyridine, 115 °C, 99%; (g) DMDO, acetone, H_2O, 0 °C, 98%; (h) Amberlyst 15, H_2O, 100 °C, 41%; DTBMP = 2,6-di-*tert*-butyl-4-methylpyridine, DMDO = dimethyldioxirane.

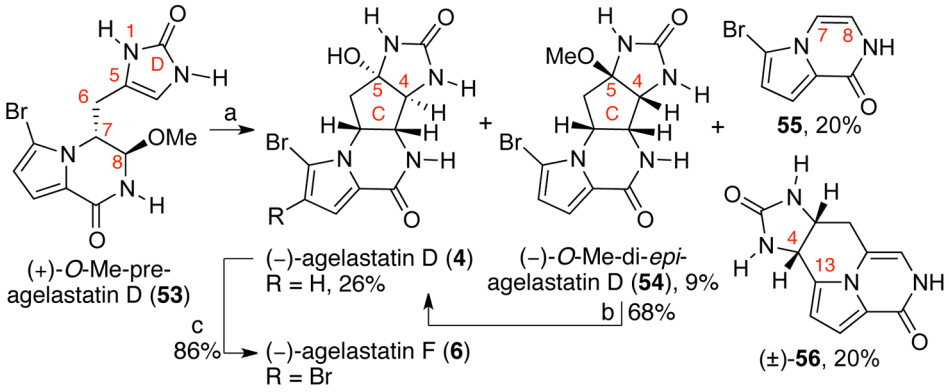

Scheme 12.

Total synthesis of (−)-agelastatin D (**4**) and the formation of byproducts **55** and **56**. Conditions: (a) $MeSO_3H$, H_2O, 100 °C; HCl, MeOH [26% (−)-**4**, 9% (−)-**54**, 20% **55**, 20% (±)-**56**]; (b) $MeSO_3H$, H_2O, 100 °C; HCl, MeOH, 23 °C, 68%; (c) NBS, DTBMP, THF, H_2O, 0 °C, 86%.

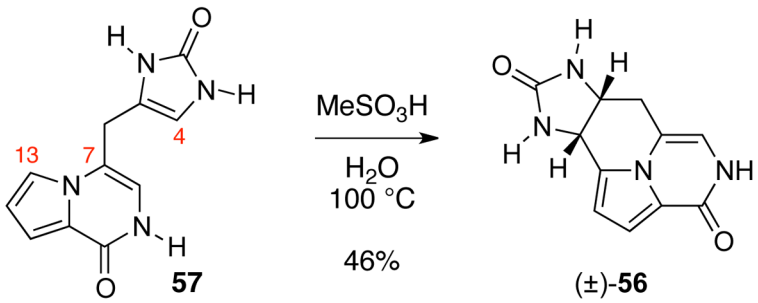

Scheme 13.
Formation of the C4–C13 bond upon acidic treatment of enamide **57**.

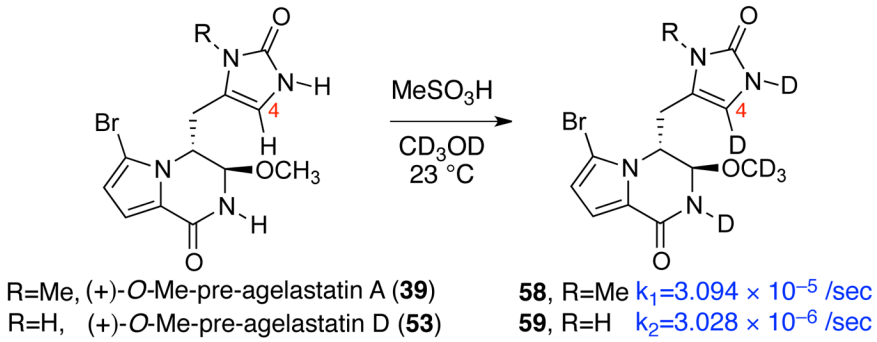

R=Me, (+)-*O*-Me-pre-agelastatin A (**39**)
R=H, (+)-*O*-Me-pre-agelastatin D (**53**)

58, R=Me $k_1=3.094 \times 10^{-5}$ /sec
59, R=H $k_2=3.028 \times 10^{-6}$ /sec

Scheme 14.
Rate constants for the deuterium incorporation at C4 of (+)-**39** and (+)-**53**.

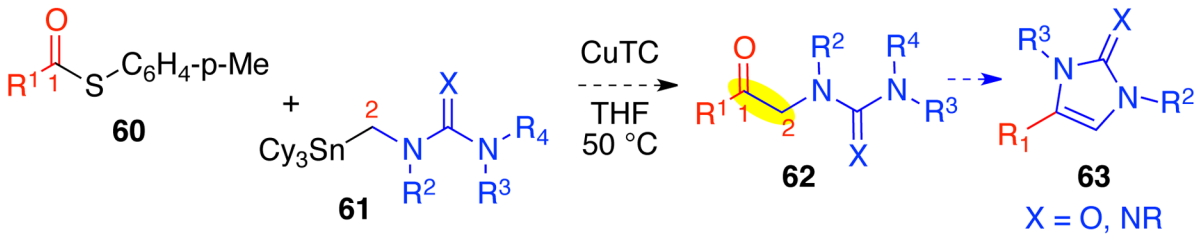

Scheme 15.
A versatile synthesis of azaheterocycle **63**.

Table 1

Copper-mediated cross-coupling between thioester (+)-**45** and stannyl triazone derivatives.

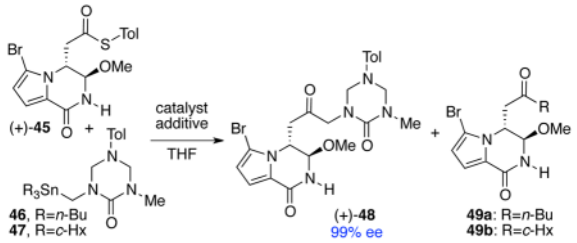

entry	triazone	catalyst (mol %)	additive (equiv)	temp (°C)	time (h)	(+)-48 (%)	49 (%)
1	**46**	$Pd_2(dba)_3$ (5)	CuDPP (2.4) $P(OEt)_3$ (0.4)	23	24	-	-
2	**46**	$Pd_2(dba)_3$ (10)	CuDPP (2.4) SPhos (0.8)	23	24	-	-
3	**46**	$Pd(PPh_3)_4$ (10)	CuDPP (2.4)	50	2	50	50
4	**46**	$Pd(PPh_3)_4$ (9)	CuTC (2.4)	50	2	60	40
5	**46**	-	CuTC (2.4)	50	1	63	36
6	**47**	-	**CuTC (1.5)**	**50**	**0.5**	**96**[a]	-

[a] Reaction was performed in >5g scale.

Tol=C_6H_4-*p*-Me, *c*-Hx=cyclohexyl, $Pd_2(dba)_3$ = tris(dibenzylideneacetone)dipalladium(0), CuDPP = copper(I)-diphenylphosphinate, SPhos = 2-dicyclohexylphosphino-2′,6′-dimethoxylbiphenyl, CuTC = copper(I)-thiophene-2-carboxylate.

Table 2

Copper-mediated thioester–aminostannane cross-coupling and application to azaheterocycle synthesis.

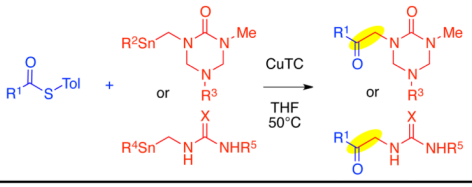

entry	thioester	stannane (equiv)	CuTC equiv	product	yield (%)
1	**64**	**47** (1.5)	1.2	**71**	95
2	**65**	**47** (1.5)	1.2	**72**	99
3	**65**	**46** (1.1)	1.5	**72**	52
4	**65**	**67** (1.1)	1.0	**73**	96
5	**65**	**67** (1.1)	1.0	**74**	96[a]
6	**66**	**67** (3.0)	2	**75**	>99
7	**66**	**67** (3.0)	2	**76**	>99[b]
8	**66**	**68** (2.5)	2.3	**77**	82
9	(+)-**45**	**69**, R=Me (3)	2.5	(+)-O-Me-pre-agelastatin A (**39**), R=Me	58[c]
10	(+)-**45**	**70**, R=H (3)	2	(+)-O-Me-pre-agelastatin D (**53**), R=H	62[d]

[a] The ketone intermediate **73** was treated with TFA in toluene at 85 °C; yield over two steps.

[b] The ketone intermediate **75** was treated with TFA in toluene at 70 °C; yield over two steps.

[c] ketone intermediate was filtered and treated with HCl in methanol at 65 °C; one step.

[d] Cross-coupling intermediate was isolated and treated with HCl in methanol at 45 °C; yield over two steps.

Tol=C_6H_4-*p*-Me, *c*-Hex=cyclohexyl.

Table 3

Assessment of the anti-cancer activity (IC_{50}) of (−)-agelastatins A–F and advanced intermediates against human cell lines after a 48-hour exposure.[a]

Cmpd	U-937 (μM)	HeLa (μM)	A549 (μM)	BT549 (μM)	IMR90 (μM)
(−)-**1**	0.067 ± 0.003	0.708 ± 0.090	1.05 ± 0.14	0.278 ± 0.076	1.11 ± 0.35
(−)-**2**	1.06 ± 0.16	4.8 ± 1.2	>10	4.8 ± 1.1	>10
(−)-**3**	>10	>10	>10	>10	>10
(−)-**4**	0.240 ± 0.033	1.00 ± 0.20	0.92 ± 0.16	0.631 ± 0.082	2.75 ± 0.60
(−)-**5**	2.56 ± 0.13	8.60 ± 0.81	>10	6.9 ± 2.5	>10
(−)-**6**	>10	>10	>10	>10	>10
(−)-**50**	>10	>10	>10	>10	>10
(−)-**51**	>10	>10	>10	>10	>10
(−)-**52**	>10	>10	>10	>10	>10
(+)-**39**	>10	>10	>10	>10	>10
(+)-**44**	>10	>10	>10	>10	>10
(+)-**45**	>10	>10	>10	>10	>10
(+)-**48**	>10	>10	>10	>10	>10
(+)-**53**	>10	>10	>10	>10	>10

[a]Cell lines: U-937, lymphoma; HeLa, cervical carcinoma; A549, non-small cell lung carcinoma; BT549, breast carcinoma; IMR90, immortalized lung fibroblasts; 48-hour IC_{50} values (in μM) as determined by MTS (U-937) and SRB (HeLa, A549, BT549, and IMR90); MTS = 3-(4,5-dimethylthiazol-2-yl)-5-(3-carboxymethoxyphenyl)-2-(4-sulfophenyl)-2H-tetrazolium); SRB = sulforhodamine B.

Table 4

48-hour activity of (−)-agelastatins A–F against human blood cancer cell lines.[a]

Cmpd	CEM (μM)	Jurkat (μM)	Daudi (μM)	HL-60 (μM)	CA46 (μM)
(−)-**1**	0.020 ± 0.002	0.074 ± 0.007	0.020 ± 0.003	0.138 ± 0.066	0.187 ± 0.071
(−)-**2**	0.29 ± 0.20	0.75 ± 0.44	0.46 ± 0.28	2.4 ± 1.0	1.07 ± 0.42
(−)-**3**	2.1 ± 1.3	5.31 ± 0.35	7.2 ± 2.9	>10	>10
(−)-**4**	0.074 ± 0.025	0.210 ± 0.063	0.202 ± 0.015	0.54 ± 0.12	0.46 ± 0.24
(−)-**5**	0.83 ± 0.37	1.50 ± 0.33	1.41 ± 0.53	4.6 ± 3.6	2.45 ± 0.95
(−)-**6**	>10	>10	>10	>10	>10

[a] Cell lines: CEM, acute lymphoblastic leukemia; Jurkat, acute T-cell leukemia; Daudi, Burkitt's lymphoma; HL-60, acute promyelocytic leukemia; CA46, Burkitt's lymphoma; 48-hour IC_{50} values (in μM) as determined by MTS; MTS = 3-(4,5-dimethylthiazol-2-yl)-5-(3-carboxymethoxyphenyl)-2-(4-sulfophenyl)-2H-tetrazolium).